The effect of Notch signaling in macrophages on metabolic diseases

Minseon Hwang

Department of Medical Science

The Graduate School, Yonsei University

The effect of Notch signaling in macrophages on metabolic diseases

Directed by Professor Kyung-Hee Chun

The Master's Thesis
submitted to the Department of Medical Science,
the Graduate School of Yonsei University
in partial fulfillment of the requirements for the degree of
Master of Medical Science

Minseon Hwang

December 2022

This certifies that the Master's Thesis of
Minseon Hwang is approved.

Thesis Supervisor : Kyung-Hee Chun

Thesis Committee Member#1 : Soo-Seok Hwang

Thesis Committee Member#2 : Seok-Jun Kim

The Graduate School
Yonsei University

December 2022

ACKNOWLEDGEMENTS

석사 학위 과정 동안 곁에서 항상 배려해주시고 응원해 주신 모든 분들께 감사 인사를 드립니다. 우선 많은 지도와 격려로 저를 이끌어주신 전경희 교수님께 큰 감사 인사를 드립니다. 부족한 저를 교수님께서 챙겨주시고 가르쳐주셔서 무사히 학위 과정을 마칠 수 있었습니다. 그리고 학위 논문을 완성하는 데에 많은 조언을 주시고 지도해 주신 황수석 교수님과 김석준 교수님께도 감사의 말씀을 드립니다. 생화학, 분자생물학 교실의 박상욱 교수님, 김경섭 교수님, 허만욱 교수님, 김건홍 교수님, 김재우 교수님, 윤호근 교수님께도 감사의 말씀을 드립니다.

짧다면 짧고, 길다면 긴 시간 동안 실험실 생활을 함께 보낸 실험실 구성원 여러분께도 감사 인사를 전합니다. 제 연구와 논문에 많은 조언과 지원을 해주신 백정환 박사님, 김명섭 박사님께 감사 드립니다. 학위 과정 동안 제 옆에 앉아 여러 도움을 주고 대화도 많이 나눴던 찬식 선생님, 항상 어려울 때마다 먼저 도와주고 정신적으로 의지할 수 있었던 졸자야 선생님, 저를 많이 챙겨준 찬호, 동기로 들어온 중권이에게 고맙다는 말을 하고 싶습니다. 앞으로의 학위 과정을 응원합니다. 선배지만 항상 저희들을 편하게 대해주시고 여러 도움을 주신 이현우 선생님, 궂은 일을 도맡아 하고 간식도 잘 챙겨주던 진선이와 유나, 함께 보낸 시간은 짧았지만 우빈이, 문규, 서희에게도 감사합니다. 지금은 다른 곳에서 자신의 꿈을 향해 열심히 노력 중인 구성원 여러분께도 감사 인사를 드립니다. 학위 과정을 시작하고 처음 저에게 여러 실험들을 가르쳐 주시고 도움을 주신 강혁구 박사님, 제가 모르는 것이 많아 물어볼 때 귀찮아 하지 않고 알려주고 도움을

줬던 재경 선생님과 창섭 선생님에게도 감사합니다. 여러분들의 도움으로 학위 과정을 무사히 마치고 이렇게 감사 인사를 전해 드릴 수 있었습니다.

생화학, 분자생물학 교실 구성원 여러분들께도 감사의 마음을 전합니다. 가까운 곳에서 도움을 주신 선영 선생님을 비롯해 항상 응원과 격려를 해주신 윤지 선생님, 예나 선생님, 다예, 루리, 규혜 선생님, 라희 선생님, 명준 선생님, 정현 선생님, 인령 선생님에게도 감사하다고 말씀 드립니다.

학위 과정 동안 옆에서 많이 응원해주고 저의 지지대가 되어준 친구들에게도 고맙습니다. 항상 제 편이 되어 응원해주고 챙겨주는 가영이와 혜원이, 멀리 있어도 잘 통하는 정아, 어리지만 때로는 언니 같은 지수, 학위 과정에 여러 조언과 격려를 해준 희정 언니와 준영 박사님, 아플 때 서로 의지한 희정 언니, 경숙 언니에게 고맙습니다. 여러분들의 응원과 지지 덕분에 학위 과정 동안 즐겁게 보내고 무사히 마칠 수 있었습니다.

마지막으로 세상에서 가장 사랑하는 가족들에게 진심으로 감사의 말씀을 드립니다. 항상 저의 선택을 존중해주시고 응원해주시는 부모님과 오빠에게 감사합니다. 곁에서 아낌없는 사랑과 응원을 주셔서 제가 지금 이 자리에 있을 수 있게 되었습니다. 건강하고 행복하게 오래도록 함께했으면 좋겠습니다. 뒤에서 묵묵히 저를 응원해주시는 할아버지와 할머니, 큰아버지, 큰어머니, 고모, 고모부, 외삼촌, 외숙모, 수경 고모께도 항상 감사 드립니다. 항상 저의 안부를 묻고 잘 챙겨주는 지수와 항상 의지가 되는 주성 오빠, 지혜 언니, 혜정 언니, 진형 오빠, 그리고 제게 웃음을 주고 힘을 주는 우리 조카들 서아, 서연, 수안이에게도 고맙고 사랑한다는 말을 전합니다. 모두 사랑합니다.

<TABLE OF CONTENTS>

LIST OF FIGURES

LIST OF TABLES

ABSTRACT

The effect of Notch signaling in macrophages on metabolic diseases

Minseon Hwang

Department of Medical Science
The Graduate School, Yonsei University

(Directed by Professor Kyung-Hee Chun)

Obesity is a chronic metabolic disease that accompanies hypertension, heart disease and type 2 diabetes. Furthermore, lipid accumulation in the adipose tissue can cause inflammation and lead to insulin resistance. Therefore, effective molecular mechanism and pharmacotherapeutic drugs need to be urgently developed to treat obesity. Although immune cells, such as macrophages, in the adipose tissue are expected to play an important role in homeostatic regulation, the mechanism by which lipids shape the phenotype of adipose tissue macrophages in diet-induced obesity remains unknown. The association between the Notch signaling system, which regulates various cell functions, and the inflammatory state is supported by many studies. Notch signaling is regulated by inflammatory signals. Hairy and enhancer of split-1 (Hes1) is a representative targets of the Notch signaling system. Hes1 negatively modulates macrophage Toll-Like Receptor (TLR) responses, suggesting that it is involved in autoimmune and inflammatory disorders. Therefore, I hypothesized that there is an association between Hes1, macrophages, and adipose tissues in relation to obesity and inflammation.

In this paper, I confirmed an increase in Notch signaling factors in the

immune cells of obese mice. When Hes1 macrophage-specific knock-out mice were fed a high-fat diet, the conditional knockout (cKO) mice gained less weight and exhibited reduced blood sugar levels. Moreover, the IL-10 expression level in bone marrow-derived macrophages (BMDMs) of the cKO mice was increased when they were in contact with adipocytes. IL-10 suppressed adipogenesis and lipid accumulation in adipocytes. I also found that tschimganidine, a terpenoid from the Umbelliferae family, inhibited Notch signaling factors and Hes1 in macrophages. Treatment with tschimganidine reduced lipid accumulation and adipogenesis accompanied by reduced expression levels of adipogenesis and lipid accumulation-related factors through AMP-activated protein kinase (AMPK) activation. These results suggest that, Hes1 in macrophages plays an important role in the adipose tissue and appears to affect metabolic diseases. Hes1 may thus be a therapeutic target for obesity and metabolic diseases. Moreover, tschimganidine, an inhibitor of Hes1, may act as an anti-obesity agent that can impede adipogenesis and improve glucose homeostasis.

Key words : Obesity, Notch signaling, Hes1, Macrophage, Natural Product

The effect of Notch signaling in macrophages on metabolic diseases

Minseon Hwang

Department of Medical Science
The Graduate School, Yonsei University

(Directed by Professor Kyung-Hee Chun)

I. INTRODUCTION

The rise in obesity and obesity-related metabolic diseases has caused an epidemic worldwide[1]. In the United States, over 78 million adults are obese and have comorbidities[2]. Obesity has been identified to be a cause of metabolic diseases, such as type 2 diabetes mellitus, nonalcoholic fatty liver disease (NAFLD), and cardiovascular disease[3]. In particular, obesity is characterized by chronic low-grade inflammation of the adipose tissue[4]. The inflammatory state in obesity is initiated and regulated by the accumulation of and change in inflammatory cells in adipose tissue[5]. As chronic adipose tissue inflammation induces insulin resistance in adipocytes and inhibits the function of storing excess energy in the adipose tissue, inflammation of the adipose tissue has been suggested to be a pathophysiological mechanism underlying the development of comorbid metabolic diseases, such as type 2 diabetes and cardiovascular disease, in individuals with obesity[4]. Therefore, it is very important to elucidate the underlying molecular mechanisms to resolve obesity and inflammation of the adipose tissue and develop therapeutic agents for preventing and managing

obesity and obesity-related metabolic diseases.

Adipose tissue macrophages (ATMs) are the most abundant immune cells in the adipose tissue. They play a key role in diet-induced type 2 diabetes mellitus and insulin resistance[6]. Macrophages in the adipose tissue can reduce the level of cytotoxic lipids by participating in lipid metabolism and lipid-mediated inflammatory responses in the adipose tissue[7, 8]. However, the mechanism by which lipids shape the phenotype of adipose tissue macrophages in diet-induced obesity remains unclear.

The Notch signaling system is present in most animals[9]. Mammals have four Notch receptors (Notch1-4), which can bind to various ligands, such as delta-like (DLL1, 3, 4) and Jagged (Jagged 1 and 2) ligands. These ligands induce the cleavage of the Notch intracellular domain (NICD) by γ-secretase and allow the NICD to migrate into the nucleus[9]. In the nucleus, the NICD interacts with recombination signal binding protein for immunoglobulin kappa J region (RBP-J), a transcriptional factor, to transcribe transcriptional repressors, such as those belonging to the Hairy and enhancer of split (Hes) family or Hairy/enhancer-of-split related with YRPW motif (Hey) family [10]. Although NOTCH1 present in this signal transduction system is known to be related to adipogenesis and lipid accumulation[11], details regarding the molecular mediators that cause this phenomenon remain unknown.

In addition to adipogenesis, the Notch signaling system has recently been shown to play an important role in immune cells and their function[12]. So far, active Notch signaling has been observed in various inflammatory conditions, including rheumatoid arthritis[13], and has been reported to be involved in the activation and function of T cells and B cells[14, 15]. The association between the Notch signaling system and the inflammatory state is supported by more and more studies, and the Notch signaling system is reported to be regulated by inflammatory signals[12]. However, the mechanism by which inflammation regulates Notch signaling is still not fully understood.

To discover a drug with an effect similar to that of the Notch signaling system on obesity and metabolic diseases, natural compound-derived therapeutic agents have been studied. Natural compound-derived therapeutics consist of bioactive phytochemicals with beneficial health effects that may be useful for treating obesity and metabolic diseases[16]. These therapeutic agents are based on substances extracted from natural sources, such as animals, plants, and minerals; therefore, they are popular as sources of medicine and as alternative treatments to prescription drugs because of the experience of using natural products for a long time and the expected effectiveness, despite controversy over their safety[17-19]. In fact, approximately 25% of medicines sold at present are derived from plants[18]. Natural products have several key advantages; they are biologically active and are composed of proteins selected by nature for specific biological interactions[20]. Natural products can be derived from secondary metabolites produced to aid the survival of organisms; hence, they exhibit low mammalian toxicity[21]. Herbal secondary metabolites also contain phytochemicals with beneficial therapeutic effects (e.g., alkaloids, terpenoids, and phenolics)[18]. Therefore, they are used in various ways to prepare nutritional supplements, dietary supplements, and genetically modified foods[16]. Moreover, several natural product-based drugs have been developed to enhance human health and alleviate cancer, cardiovascular disease, and osteoporosis[16].

While studies conducted so far have suggested some link between the Notch signaling system, fat accumulation, and immune cells in the adipose tissue, certain molecular mechanisms remain questionable. In addition, the physiological relationship between Hes1, which is a representative target of the Notch signaling system, and macrophages has not been revealed. Based on these points, I first hypothesized that Hes1 deficiency would ameliorate metabolic diseases such as obesity and fatty liver disease. Moreover, I intended to conduct a study on the physiological effect of Hes1 on lipid accumulation and macrophage in adipose tissue through this study. I also aimed to search for

a drug that has an effect similar to that of the notch signaling system on the adipose tissue.

II. MATERIALS AND METHODS

1. Mice

Wild-type C57BL6/J male mice were purchased from Orient Bio Inc. (Gyeonggi, Republic of Korea). $Hes1^{fl/fl}$ mice (kindly provided by Young-Yun Kong at Seoul National University, Seoul, Korea) were bred with LysM-Cre^{+} mice (kindly provided by Heung Kyu Lee at KAIST, Daejeon, Korea). Age and sex-matched cohorts of female (8–12 weeks old) and males (8–12 weeks old) littermates were used for isolation of BMDMs. Seven-week-old wild-type and Hes1 conditional Knockout (cKO) mice were fed a high-fat diet (HFD, chow diet, 60% of the total kcal as fat, Research Diets, Inc; New Brunswick, NJ, Canada) for 10–12 weeks (12-h light/12-h dark cycle).

The mice were intraperitoneally injected with 1 and 5 μg/kg of tschimganidine (Enzo Life Sciences, NY, USA). To assess metabolic parameters, eight-week-old mice were fed either a normal chow diet (NFD) or a HFD with or without tschimganidine for 12 weeks. Body weight and food intake were measured every two days to evaluate the effect of tschimganidine treatment.

All mouse tissues (gonadal white adipose tissue [gWAT], inguinal white adipose tissues [iWAT], liver tissue, and brown adipose tissue [BAT], among others) were frozen in liquid nitrogen and stored at -80 ℃ until analysis. All animal studies were approved by the Institutional Review Board of the Yonsei University College of Medicine and were performed in specific pathogen-free facilities according to the Guidelines for the Care and Use of Laboratory Animals (2018-0289).

2. Cell culture and adipocyte differentiation

THP-1 cells were cultured in Rosewell Park Memorial Institute (RPMI)-1640 medium with 10 % fetal bovine serum (FBS) and 1% penicillin/streptomycin

(P/S) and stimulated with phorbol 12-myristate 13-acetate (PMA, 100 nM, Sigma-Aldrich, St. Louis, MO, USA) for differentiation.

3T3-L1 cells were maintained and grown to a post-confluency state using Dulbecco's modified Eagle's medium (DMEM) supplemented with 10% bovine serum. On day 0 post-confluence, the 3T3-L1 cells were incubated in DMEM supplemented with 10% FBS, insulin (1 μg/mL, Sigma-Aldrich, St. Louis, MO, USA), isobutylmethylxanthine (IBMX, 520 mM, Sigma-Aldrich, St. Louis, MO, USA), and dexamethasone (1 μM, Sigma-Aldrich, St. Louis, MO, USA). After two days, the medium was replaced with DMEM supplemented with 10% FBS and insulin (1 μg/mL). After four days, the medium was replaced with DMEM supplemented with 10% FBS.

3. Preparation of BMDMs

Genotype-, age-, and sex-matched cohorts of male or female mice aged six to 12 weeks were euthanized, and both femurs were dissected free of adherent tissue. Bone marrow cells from femur and tibia were subjected to red blood cell lysis using red blood cell lysis buffer, and the surviving cells were cultured for six days in differentiation medium. On day 3, 5 ml of medium was added. The differentiation medium consisted of DMEM and 10% FBS with 20ng/ml macrophage colony-stimulating factor (M-CSF, Peprotech, NJ, USA). P/S was also added to the medium. Cells were harvested with cold phosphate-buffered saline (PBS), washed, resuspended in DMEM supplemented with 10% FBS, and used at a density of 4–10 × 10^5 cells/mL for experiments.

4. Cell viability assay

3T3-L1 cells were cultured in 12-well plates and incubated until they reached confluence. The cells were then treated with tschimganidine for 48 h at the indicated concentrations. Cell viability was measured using Ez-Cytox (Daeil Lab Co. Ltd., Seoul, Republic of Korea), according to the manufacturer's

protocol.

5. Transfection of small interfering RNA (siRNA)

THP-1 cells were cultured in a six-well plate and incubated for 24 h with stimulation using PMA. The cells were transfected with human Hes1 siRNA at 20 nM (Bionics, Seoul, Republic of Korea) using Lipofectamine™ RNAiMAX (Invitrogen, Waltham, MA, USA) according to the manufacturer's protocol. After 6 h, the medium was replaced with RPMI supplemented with 10% FBS, and 1% P/S. After 2 days, the cells were harvested.

3T3-L1 cells were cultured in a six-well plate and incubated for 24 h. The cells were transfected with mouse AMP-activated protein kinase catalytic subunit alpha-1 (AMPKa1) siRNA at 50 nM (Bionics, Seoul, Republic of Korea) using Lipofectamine™ RNAiMAX according to the manufacturer's protocol. After 24 h, the medium was replaced with DMEM supplemented with 10% bovine serum. On next day, cell differentiation was induced by transferring the cells to DMEM supplemented with 10% FBS, insulin (1 μg/mL), IBMX (520 μM), and dexamethasone (1 μM).

6. Western blot analysis

Cell lysate extractions were performed using radio-immunoprecipitation assay (RIPA) buffer (1% Triton X-100; 1% sodium deoxycholate; 0.1% sodium dodecyl sulfate; 150 mM NaCl; 50 mM Tris–HCl, pH 7.5; and 2 mM EDTA, pH 8.0). The lysates were briefly vortexed and cleared by centrifugation at 13,200 rpm for 20 min at 4℃. The supernatant was transferred to a new microcentrifuge tube. The concentration of protein in the supernatant was measured using a protein assay reagent (Thermo Scientific, Waltham, MA, USA). In total, 20–50 μg of total protein in each lysate was resolved in SDS PAGE gels and electrotransferred to PVDF membranes (Merck Millipore, Billerica, MA, USA). The membranes were blocked with 2% skim milk in

PBST buffer for 1 h at room temperature. The following primary antibodies were used: antibodies against Jagged 1, Jagged 2, C/EBPα, PPARγ, FABP4, FASN, phosphorylated (p)-AMPK, AMPK, p-AKT, AKT, p-JAK2, and JAK2 from Santa Cruz Biotechnology (Dallas, Texas, USA) and antibodies against Hes1, Hey1, NOTCH1, NOTCH3, NOTCH4, DLL4, p-ACC, ACC, p-ERK1/2, and ERK1/2 from Cell Signalling (Danvers, MA, USA). The membranes were washed thrice for 10 min. The FUSION Solo S (Vilber, Paris, France) was used for image detection, according to the manufacturer's instructions. The normalization control used was anti-β-actin (Santa Cruz Biotechnology, Dallas, Texas, USA).

7. RNA isolation, reverse transcription and real-time PCR analysis

RNA was isolated using TRIzol reagent (Invitrogen, Carlsbad, CA, USA), according to the manufacturer's instructions. cDNA (1–4 μg) was synthesized using a reverse transcription-PCR (RT-PCR) master mix (TOYOBO, Tokyo, Japan). RT-PCR was performed using a reverse transcription system (TOYOBO, Tokyo, Japan). Real-time PCR was performed using the instructions provided in TB Green Premix EX Taq (TaKaRa, Kyoto, Japan) with ABI instruments (Applied Biosystems Inc, Foster City, CA, USA). All results were normalized by β-actin. The primers are listed in Table 1.

8. Oil Red O staining

Differentiated 3T3-L1 cells were washed with PBS, incubated in 10% formalin for 10 min, and washed with distilled water. The cells were then stained with ORO (Sigma-Aldrich, St. Louis, MO, USA) in 60% isopropanol for 1 h. The stain retained by the cells was eluted with 100% isopropanol, and OD_{500} of the solution was measured with a microplate reader (Molecular Devices, CA, USA).

9. Analysis of serum metabolic parameters

Blood was collected from the mice as mentioned above and centrifuged for 10 min at 132 ×g to obtain serum. Serum analysis, including assessment of alanine aminotransferase (ALT), glucose, triglyceride (TG), total cholesterol, and free fatty acid (FFA) contents, was performed at the Seoul Medical Science Institute, Gyeonggi, Republic of Korea.

10. Metabolic assays

Glucose tolerance tests (GTTs) were performed by intraperitoneal injecting mice with 1 g/kg glucose (Sigma-Aldrich, St. Louis, MO, USA). Insulin tolerance tests (ITTs) were performed by intraperitoneal injecting mice with 1 U/kg insulin (Humulin). Blood glucose levels were measured 0, 15, 30, 60, 90, and 120 min after injection using a glucometer.

11. Morphological analysis of tissues

gWAT, iWAT, liver tissue, and BAT were fixed in 4% paraformaldehyde for 24–48 h at 4℃, processed for paraffin embedding, and stained with hematoxylin and eosin (H&E). The cell size was analyzed using ImageJ software[22].

12. Quantification of hepatic triglycerides and free fatty acids

Hepatic TG content was measured in lipid extracts from previously frozen liver tissues of mice fed a NFD or HFD with or without tschimganidine for 12 weeks using the Triglyceride Quantification Colorimetric Kit (BioVision, Mountain View, CA, USA), following the manufacturer's instructions. Colorimetric measurements were performed at 570 nm using a microplate reader (Molecular devices, CA, USA). Similarly, Hepatic FFA content was measured in lipid extracts from previously frozen liver tissues using the FFA Quantification Colorimetric Kit (K612-100, BioVision, Mountain View, CA,

USA), following the manufacturer's instructions. Colorimetric measurements were performed at 570 nm using microplate reader (Molecular devices, CA, USA). All experiments were performed at least thrice.

13. Flow cytometry

Single-cell suspensions were prepared from adipose tissues. Adipose tissues were extracted and processed as described above before resuspension in PBS buffer containing 2% FBS 20 and 2mM EDTA for flow cytometric analysis. The LIVE/DEAD^{TM} Fixable Near-IR Dead Cell Stain Kit (L10119, Invitrogen) was used in combination with anti-mouse CD16/CD32 Fc blocker antibody (#14-0161-81, Invitrogen) for 15 min on ice in the dark. The cells were washed and incubated with fluorochrome-conjugated antibody (anti-mouse F4/80 PerCP/Cy5.5, clone BM8, Biolegend cat. 123127; anti-mouse CD11b FITC, clone M1/70, Biolegend cat. 1001206) at the manufacturer-recommended dilution for 30 min on ice in the dark. The cells were washed with PBS and resuspended in FACS buffer for flow cytometric analysis on BD LSRFortessa at the Flow Cytometry Core of the Abision Biomedical Research Center, Yonsei College of Medicine. In total, 10,000–1,000,000 cells were analyzed per sample using BD FACS Diva Software. The data was analyzed using Flow Jo software.

14. Statistical analysis

Data were plotted and statistically analyzed using Prism 5 (Graph-Pad, San Diego, CA, USA) and presented as the mean ± SD or SEM. Unpaired t-tests were used to compare the two groups. Statistical significance was set at $P < 0.05$.

Table 1. Primer lists and sequences for RT-PCR

Primer	Sequence (5' to 3')
β-actin	Forward: GGCTGTATTCCCCTCCATCG
	Reverse: CCAGTTGGTAACAATGCCATGT
Notch1	Forward: TGAGAATGATGCCCGCACTT
	Reverse: CAGGTGCCCTGATTGTAGCA
Notch2	Forward: AGCAGGAGCAGGAGGTGATA
	Reverse: TGGGCGTTTCTTGGACTCTC
Notch3	Forward: CAGGCGAAAGCGAGAACAC
	Reverse: GGCCATGTTCTTCATTCCCA
Notch4	Forward: ATGACTCCTTGCCCTCTCTCT
	Reverse: CTCTCACCCTTTAGTCCCTCAGA
Hes1	Forward: ACACCGGACAAACCAAAGACA
	Reverse: AATGCCGGGAGCTATCTTTC
Hes2	Forward: TCAACGAGAGCCTAAGCCAGCT
	Reverse: CGCACAGTCATTTCCAGGATGTC
Hes5	Forward: AGTCCCAAGGAGAAAAACCGA
	Reverse: GCTGTGTTTCAGGTAGCTGAC
DLL1	Forward: CGGGCCAGGGGAGCTACACA
	Reverse: AGCTGTCCTCAAGGTCCGTGG
DLL4	Forward: CAGCATCCCCTGGCAGTGTGC
	Reverse: GCTGGCACACTTGCTGAGTCCC
HEY1	Forward: GCCGAAGTTGCCCGTTATCTG
	Reverse: TGTGTGGGTGATGTCCGAAGG
PPARγ	Forward: GATGCACTGCCTATGAGCAC
	Reverse: TCATGGAGAGGTCCACAGAG

C/EBPα	Forward: GACATCAGCGCCTACATCGA
	Reverse: TCGGCTGTGCTGGAAGAG
FABP4	Forward: CATCAGCGTAAATGGGGATT
	Reverse: TCGACTTTCCATCCCACTTC
FASN	Forward: TGGGTTCTAGCCAGCAGAGT
	Reverse: ACCACCAGAGACCGTTATGC
Jagged 1	Forward: CATGCTCCAATCCACGGAGTA
	Reverse: CAGGGCGAGCAGAAGACTCA
Jagged 2	Forward: CTGGGTGGCAACTCCTTCTA
	Reverse: AGCTCCTCATCTGGAGTGGT
IL-10	Forward: ATAACTGCACCCACTTCCCA
	Reverse: GGGCATCACTTCTACCAGGT
Human β-actin	Forward: AGCCTCGCCTTTGCCGA
	Reverse: CTGGTGCCTGGGGCG
Human Hes1	Forward: ATGGAGAAAAATTCCTCGTCCC
	Reverse: TTCAGAGCATCCAAAATCAGTGT
Human IL-10	Forward: ATGCACAGCTCAGCACTGCTCTG
	Reverse: CTTAAAGTCCTCCAGCAAGGACTCC

III. RESULTS

1. Notch signaling of ATMs is activated under HFD conditions and upon contact with adipocytes

When the NCD- and HFD-fed mice were analyzed with FACS, the macrophage population in the stromal vascular fraction (SVF) in the epididymal white adipose tissue (eWAT) increased under HFD conditions (Fig. 1A). Moreover, the mRNA level of Notch signaling factors, including Hes1, was elevated in ATMs of HFD-fed mice (Fig. 1B and 1C). Using the co-culture system with differentiated adipocytes, I observed whether adipocytes or lipids affect macrophages. Notch signaling was activated when BMDMs contacted adipocytes (Fig. 1D). This result is consistent with the finding that Notch signaling is activated in ATMs. These results suggest that Hes1, an activated Notch signaling target of macrophages, is associated with obesity and inflammatory responses in the adipose tissue.

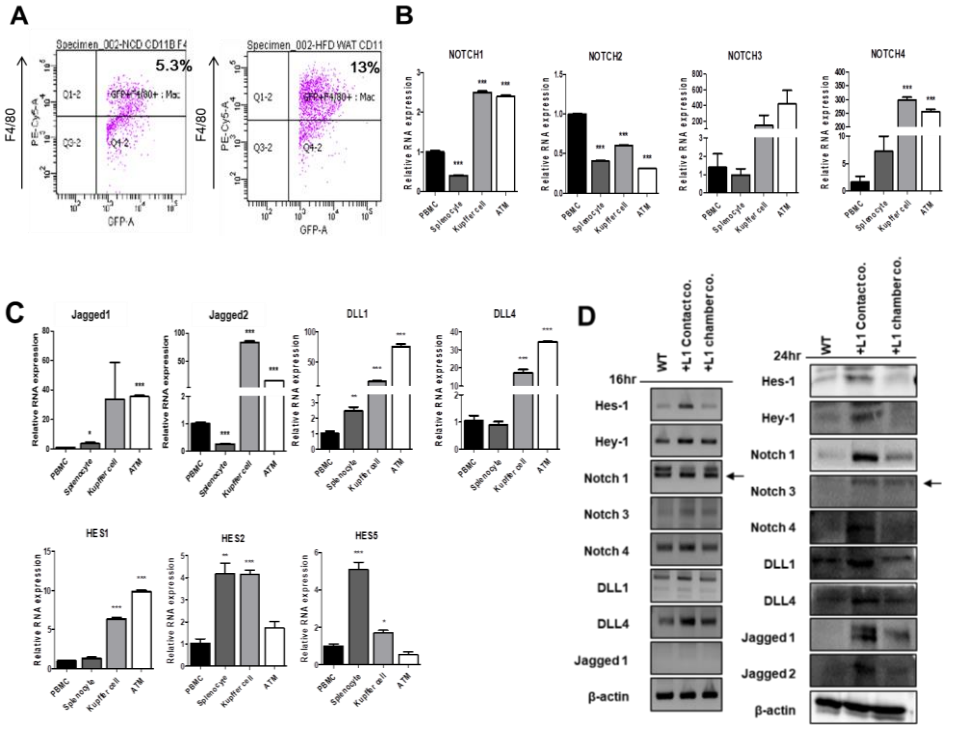

Figure 1. Notch signaling of ATM is activated in high fat diet condition. (A) Representative flow cytometry analysis of F4/80 and green fluorescent protein (GFP) expression in the SVF of eWAT from normal chow diet-fed LysM cre-GFP mice and high-fat diet-fed LysM cre-GFP mice. (B, C) mRNA expression of Notch signaling and Hes1 in tissue macrophages from WT mice. β-actin was used as a loading control for real-time PCR analysis. **P* < 0.05, ** *P* <0.01 and *** *P* <0.001. (D) mRNA expression of Hes1, Hey1, Notch1, Notch3, Notch4, DLL1, DLL4 and Jagged 1 in WT mouse BMDMs and BMDMs co-cultured with differentiated 3T3-L1 cells. β-actin was used as a loading control for RT-PCR analysis. Protein expression of Hes1, Hey1, Notch1, Notch3, Notch4, DLL1, DLL4 and Jagged 1, and Jagged 2 in WT mouse BMDMs and BMDMs co-cultured with differentiated 3T3-L1 cells was detected by western blotting. Protein expression was normalized to β-actin.

2. Inhibition of Hes1 expression in macrophages ameliorates obesity in HFD fed mice

To identify the role of Hes1 in mouse macrophages, cKO of Hes1 genes was performed using LysM–Cre–LoxP recombination, which specifically affects myeloid cells. This model was fed a HFD to induce obesity. After 12 weeks, the Hes1 cKO mice had significantly lower body weight than the wild-type mice; however, no difference was noted in the body weight of the NFD-fed groups (Fig. 2A and 2B). Compared with the control group, fat and free body fluid accounted for a lower proportion of the body composition in the Hes1 cKO mice, while lean tissue accounted for a higher proportion of the body composition under HFD conditions (Fig. 2C). To determine whether the deletion of Hes1 in macrophages affects the metabolic fitness, voiding behavior of the mice was assessed using a metabolic cage system. The oxygen composition (VO_2), respiratory exchange ratio (RER) and energy expenditure (EE) increased in the Hes1 cKO mice. The Hes1 cKO mice consumed more food but performed less activity. Next, histological analysis of adipose and liver tissues of HFD-fed mice was performed. The gWAT, iWAT, and BAT of the Hes1 cKO mice were drastically reduced compared with those of the wild-type mice. Moreover, the Hes1 cKO mice had significantly smaller adipocyte sizes, as revealed by H&E staining (Fig. 2D, 2E and 2F). The weight of the liver was similar between the two groups; however, the size of lipid droplets was lower in the liver of the Hes1 cKO mice (Fig. 2G). Following histological analysis, the metabolic characteristics of Hes1 was assessed in HFD-fed mice. GTTs and ITTs were performed to identify the role of Hes1 in glucose metabolism. Blood glucose levels over the entire testing period were lower in the Hes1 cKO mice (Fig. 2H). Also, blood serum samples of these mice were analyzed. ALT, blood glucose, total cholesterol, and FFA contents were lower in the Hes1 cKO mice (Fig. 2I). These data imply that Hes1 deletion in macrophages ameliorates obesity under HFD conditions.

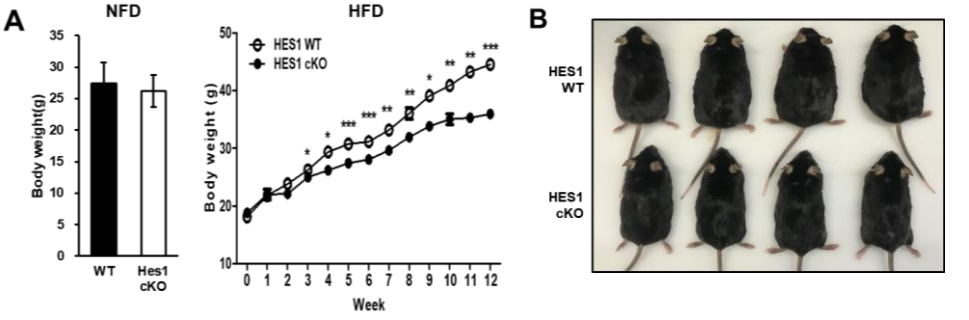

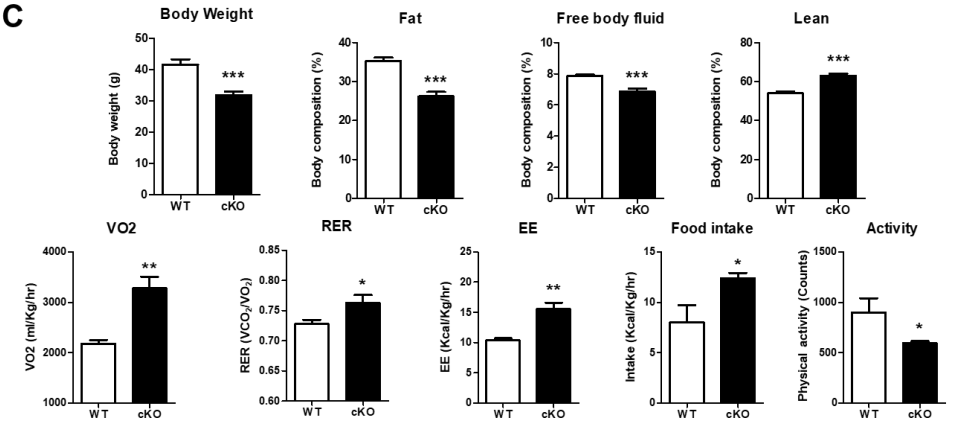

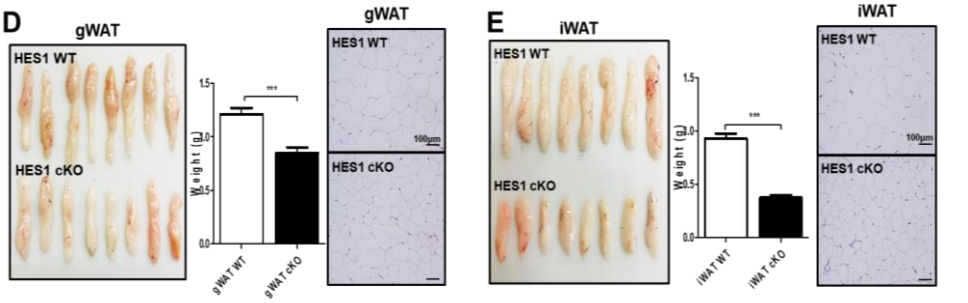

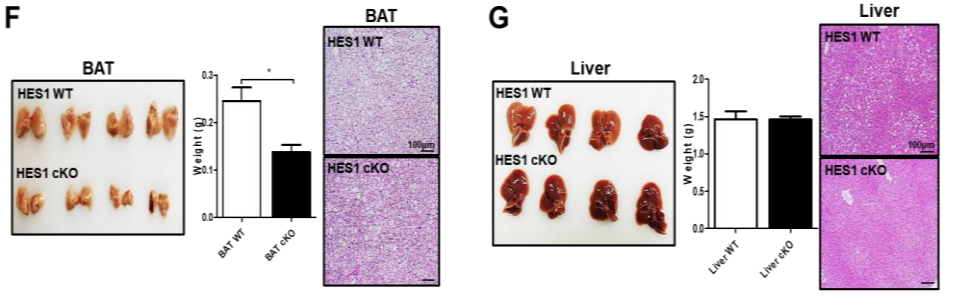

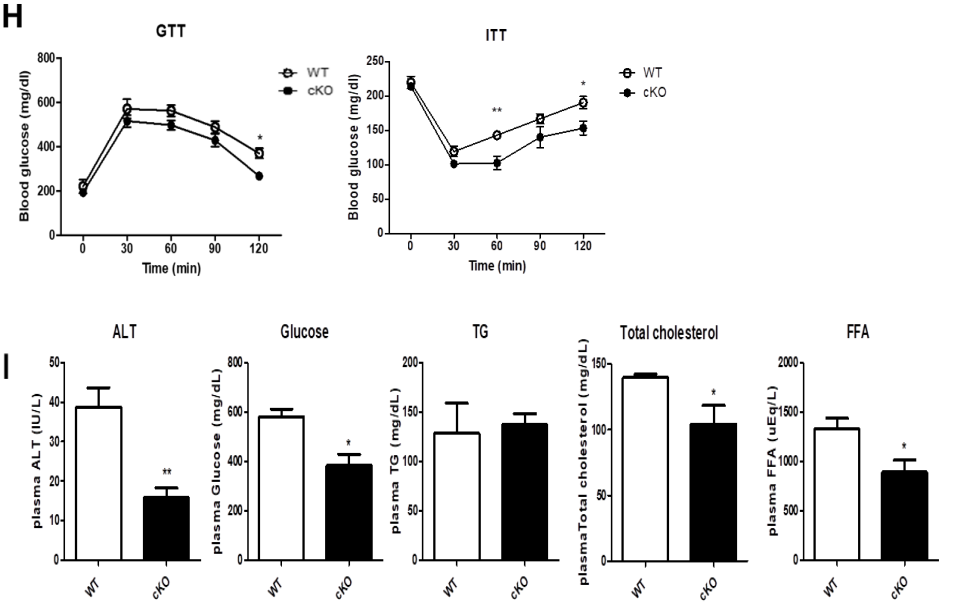

Figure 2. Inhibition of Hes1 expression in macrophages ameliorates obesity in high-fat diet-fed mice. Adiposity and weight gain in WT and HES1-LysM cKO mice. (A, B) Body weight of male WT and Hes1 macrophage cKO mice fed a NFD or HFD was measured over 12 weeks (n = 12 to 15). (C) Metabolic characteristics of mice. Body weight gain, body composition, oxygen consumption, energy expenditure, food intake, and movement in WT mice and HES1-LysM cKO mice fed a HFD. *P < 0.05, ** P <0.01, and ***P <0.001 versus WT; unpaired t test. (D–G) White adipose tissue, BAT, and liver tissue from HFD-fed WT and Hes1 cKO mice. Each tissue weight was measured after the 12-week dietary period. The adipocyte size in each tissue section was measured by H&E staining. Size measurements were performed using ImageJ software. (H) Blood glucose profiles during intraperitoneal GTT (Left); Blood glucose profiles during intraperitoneal ITT (Right). The results are expressed as the mean ± S.E.M. (n = 4–7/group). (I) Serum levels of the indicated lipid metabolites. For statistical analysis, means and SEM were determined (n = 7 for

each group). *P < 0.05, **P < 0.01, NS, statistically not significant. NFD, normal-fat-diet; HFD, High-fat-diet; BAT, Brown adipose tissue; H&E, hematoxylin and eosin; GTT, glucose tolerance test; ITT, insulin tolerance test.

3. Hes1 cKO macrophages increase IL-10 expression upon contact with adipocytes, and IL-10 suppresses adipogenesis in adipocytes

I determined how macrophage-specific Hes1 knockout induces an anti-obesity effect. First, BMDMs from wild-type and Hes1 cKO mice were separately cultured with differentiated 3T3-L1 cells using a direct interaction system. Their gene expression levels were analyzed by RNA sequencing. upon contact with differentiated adipocytes, it was confirmed that the IL-10 gene expression level was higher in the Hes1 cKO BMDMs than in the control BMDMs (Fig. 3A). This result was reconfirmed by real-time PCR analysis (Fig. 3B). IL-10 gene expression was also increased in THP-1 cells by the knockdown of Hes1 gene expression using Hes1 siRNAs (Fig. 3C). IL-10 is a marker of M2 macrophages and is one of the cytokines secreted by ATMs in the physiological state of obesity[23]. M2 macrophages induce insulin sensitivity through the anti-inflammatory actions of IL-10[23]. These results suggest that Hes1-inhibited macrophages in the adipose tissue express more IL-10, thereby reducing the inflammatory response. Next, I assessed whether IL-10 suppresses adipogenesis and lipid accumulation. Two days after methylisobutylxanthine–dexamethasone–insulin (MDI) induction, 3T3-L1 cells were treated with different concentrations of IL-10 for 24 h. IL-10 treatment reduced the mRNA (Fig. 3D) and protein (Fig. 3E) expression levels of adipogenesis-related genes, particularly those encoding PPARγ and its downstream factors, C/EBPα, FABP4, and FASN. ORO staining revealed that IL-10 inhibited lipid accumulation in adipocytes in a dose-dependent manner on day 6 (Fig. 3F). 3T3-L1 cells were treated with IL-10 (10 ng/ml) at each stage of adipocyte differentiation. IL-10 effectively reduced the protein expression of adipogenesis-related factors when treated on day 2 or throughout the differentiation phase (Fig. 3G). Collectively, these data suggest that Hes1 inhibition increases the expression level of IL-10 with an anti-inflammatory effect in macrophages and that IL-10 reduces adipogenesis in adipocytes.

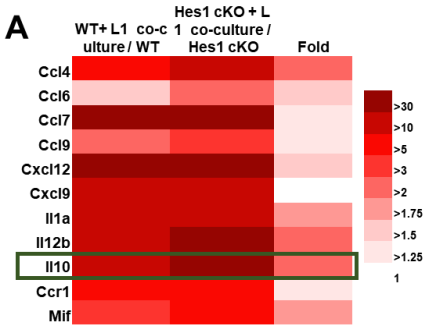

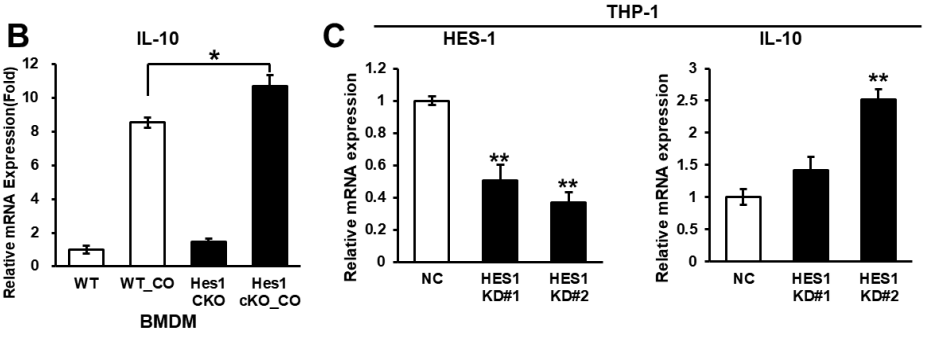

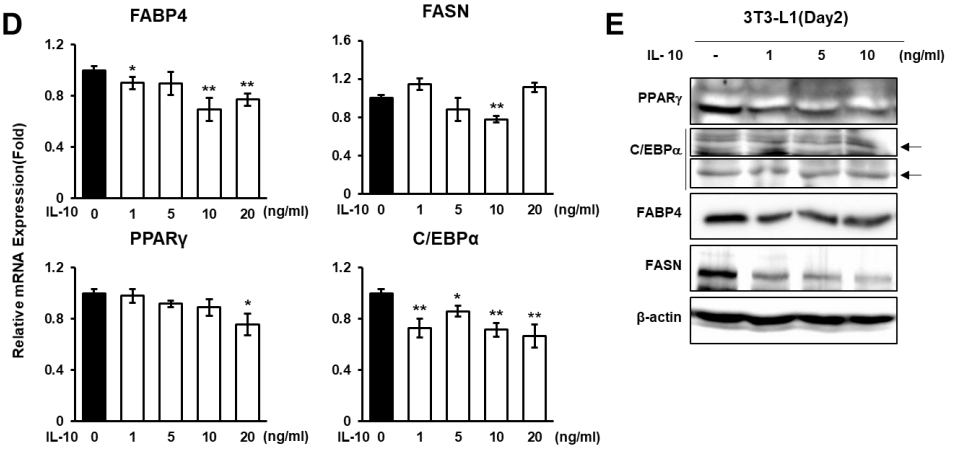

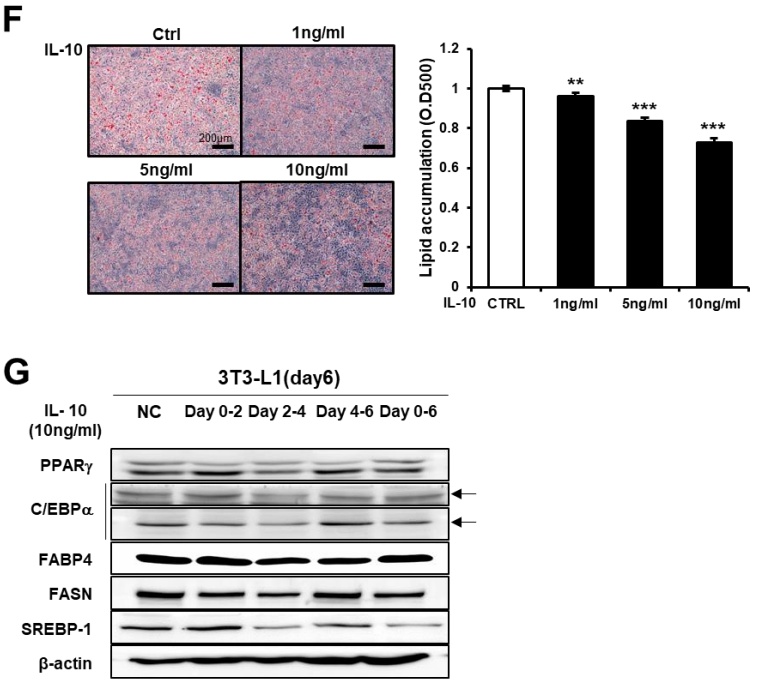

Figure 3. Hes1 cKO macrophages increase IL-10 expression, and IL-10 suppresses adipogenesis in adipocytes. (A) For each sample pair, the WT + L1: WT ratio, Hes1 cKO + L1:Hes1 cKO ratio, and Hes1 cKO + L1/Hes1 cKO: WT+L1/WT ratios were calculated using gene expression levels obtained by bulk RNA sequencing. Each RNA sample was extracted from WT or Hes1 cKO mouse BMDMs and WT or Hes1 cKO BMDMs co-cultured with differentiated 3T3-L1 cells. (B) Detection of mRNA expression of IL-10 in macrophages from WT or Hes1 cKO mouse BMDMs and WT or Hes1 cKO BMDMs co-cultured with differentiated 3T3-L1 cells. β-actin was used as a loading control for real-time PCR. $*P < 0.05$. (C) mRNA expression of Hes1 and IL-10 in THP-1 cells was detected using real-time PCR. RNA samples were prepared after Hes1 knock down using Hes1 siRNAs. mRNA expression was normalized to that of β-actin. $*P < 0.05$, $**P < 0.01$. (D) mRNA expression of PPARγ, C/EBPα, FABP4, and FASN was detected using real-time PCR. RNA samples

were prepared on days 3. 3T3-L1 cells were treated with IL-10 at the indicated concentrations for 24 h on day 2. mRNA expression was normalized to that of β-actin. *P < 0.05, **P < 0.01. (E) Protein expression of PPARγ, C/EBPα, FABP4, and FASN was detected by western blotting. 3T3-L1 cells were treated with IL-10 at the indicated concentrations for 24 h on day 2. Protein expression was normalized to that of β-actin. (F) ORO staining of IL-10-treated 3T3-L1 cells. After MDI induction, 3T3-L1 cells were treated with IL-10 on days 2 to 6 at the indicated concentrations. ORO staining was performed on day 6. Measurement of lipid accumulation. ORO was eluted with 100% isopropanol from the stained cells, and the absorbance was measured at 500 nm. **P < 0.01, ***P < 0.001. (G) Protein expression of PPARγ, C/EBPα, FABP4, and FASN was detected by western blotting. 3T3-L1 cells were treated with IL-10 (10ng/mL) at the indicated stages. Cell lysates were prepared on days 6. Protein expression was normalized to that of β-actin. ORO, Oil Red O.

4. Tschimganidine has a similar effect to Notch signaling inhibition in macrophages

Next, I searched for a natural therapeutic agent having a similar effect on macrophages and adipocytes. Tschimganidine, a terpenoid, exhibited the expected effect; its structure is presented in Fig. 4A. Tschimganidine treatment reduced the protein expression levels of Notch signaling factors, such as Notch1, Notch3, DLL4, Hes1, Hey1, Jagged 1 and Jagged 2, but increased the protein expression level of IL-10 in BMDMs (Fig. 4B). Therefore, I confirmed whether tschimganidine inhibits adipogenesis and lipid accumulation. 3T3-L1 preadipocytes were treated with different concentrations of tschimganidine 2 days after the induction of cell differentiation in order to evaluate the effect of tschimganidine. Adipogenesis, the process by which adipocyte precursors develop into mature adipocytes, was assessed by ORO staining of the lipid droplets on day 6 (Fig. 4C). ORO staining revealed that tschimganidine reduced lipid accumulation in a dose-dependent manner. Tschimganidine treatment at 5 μg/mL reduced lipid accumulation. The tschimganidine doses that were most effective in inhibiting adipocyte differentiation and lipid accumulation were 25 and 50 μg/mL, respectively. A cell viability assay was performed to determine whether the inhibitory effect of tschimganidine on lipid accumulation resulted from cell cytotoxicity. No significant difference in cell viability was noted between tschimganidine-treated and control cells (Fig. 4D). The expression of adipogenesis-related proteins, namely PPARγ, and its downstream factors, C/EBPα, FABP4, and FASN, decreased after tschimganidine treatment in a dose-dependent manner (Fig. 4E). These results suggest that tschimganidine mimics Hes1 inhibition effects and inhibits adipogenic differentiation by downregulating the expression of adipogenesis-associated proteins.

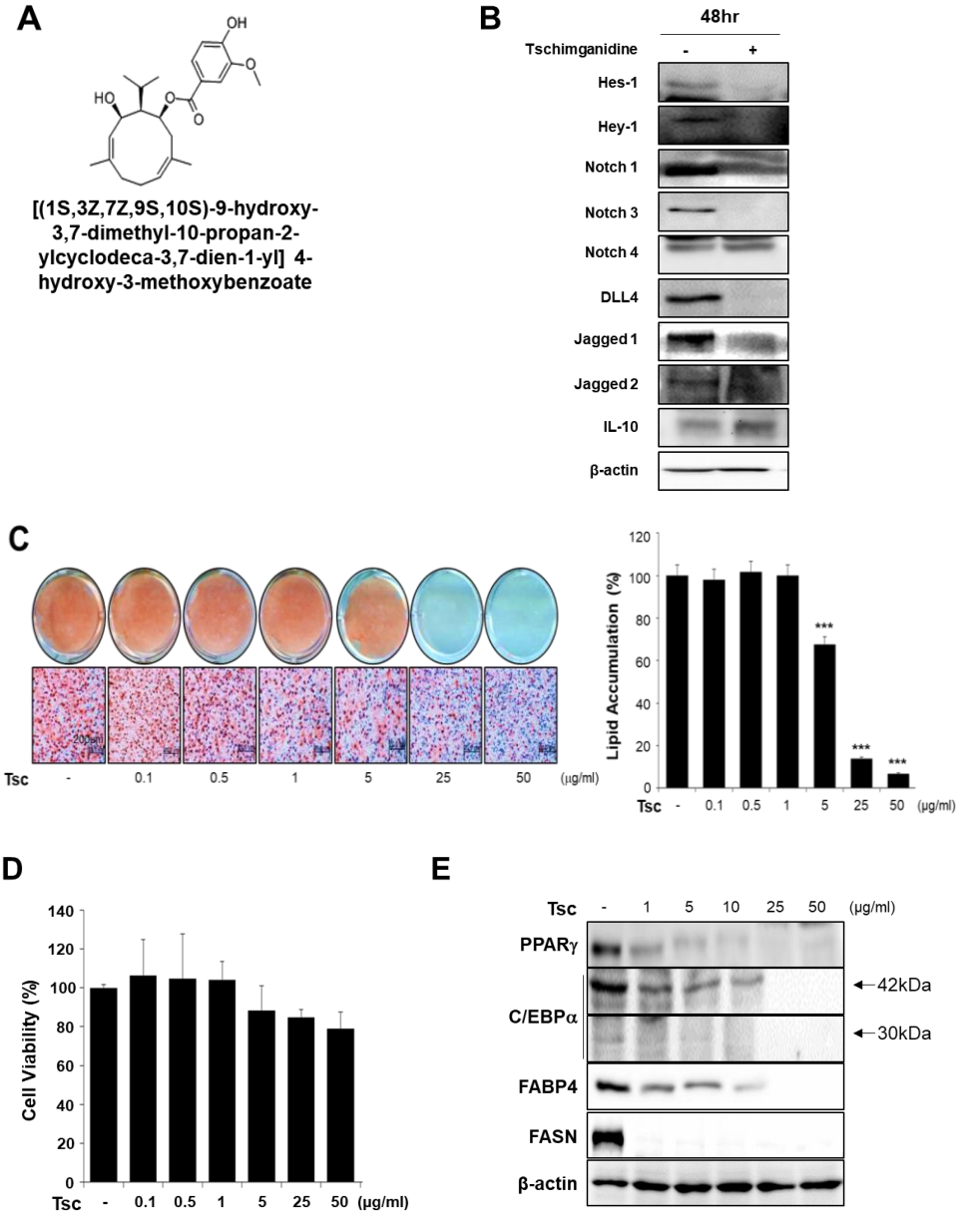

Figure 4. Tschimganidine has a similar effect to Notch signaling inhibition in macrophages. (A) Structure of tschimganidine. (B) Protein expression of Notch signaling factors in BMDMs after tschimganidine treatment for 48 h was detected by western blotting. Protein expression was normalized to that of

β-actin. (C) ORO staining of tschimganidine-treated 3T3-L1 cells. After MDI induction, 3T3-L1 cells were treated with tschimganidine on days 2 to 6. ORO staining was performed on day 6. Measurement of lipid accumulation. ORO was eluted with 100% isopropanol from the stained cells, and the absorbance was measured at 500 nm. ***P <0.001, dimethyl sulfoxide versus tschimganidine. (D) Cell viability assays. Confluent 3T3-L1 cells were treated with tschimganidine for 48 h. (E) Protein expression of PPARγ, C/EBPα, FABP4, and FASN was detected by western blotting. Protein expression was normalized to that of β-actin. ORO, Oil Red O; MDI, methylisobutylxanthine–dexamethasone–insulin.

5. Tschimganidine reduces the expression levels of adipogenesis-related factors after adipocyte differentiation

Tschimganidine (15 μg/mL) exhibited a dose-dependent inhibitory effect on lipid accumulation, as observed by ORO staining (Fig. 5A). Whole-cell lysates were obtained on days 0, 2, 4, and 6 to assess how tschimganidine treatment affects adipogenesis- and lipid accumulation-related genes during adipocyte differentiation. 3T3-L1 cells were treated with tschimganidine 2 days after adipogenic stimulation. Tschimganidine significantly suppressed the mRNA (Fig. 5B) and protein (Fig. 5C) expression of PPARγ, C/EBPα, FABP4, and FASN after 2 days of treatment. I further investigated whether the inhibitory effect of tschimganidine occurs at the early or late stages of adipogenesis. Cells were treated with MDI and tschimganidine on day 0. Tschimganidine treatment reduced adipocyte differentiation and lipid accumulation (Fig. 5D). I also assessed the effects of tschimganidine on late adipocyte differentiation. 3T3-L1 cells were incubated with tschimganidine from days 6 to 10. Compared with control cells, tschimganidine treatment reduced lipid accumulation and lipid droplet size in 3T3-L1 cells. ORO staining results revealed that tschimganidine retarded all stages of adipocyte differentiation, including the early stage (days 0 to 2) and late stage (days 6 to 10). These data indicate that tschimganidine represses adipogenesis and reduces lipid accumulation in adipocytes.

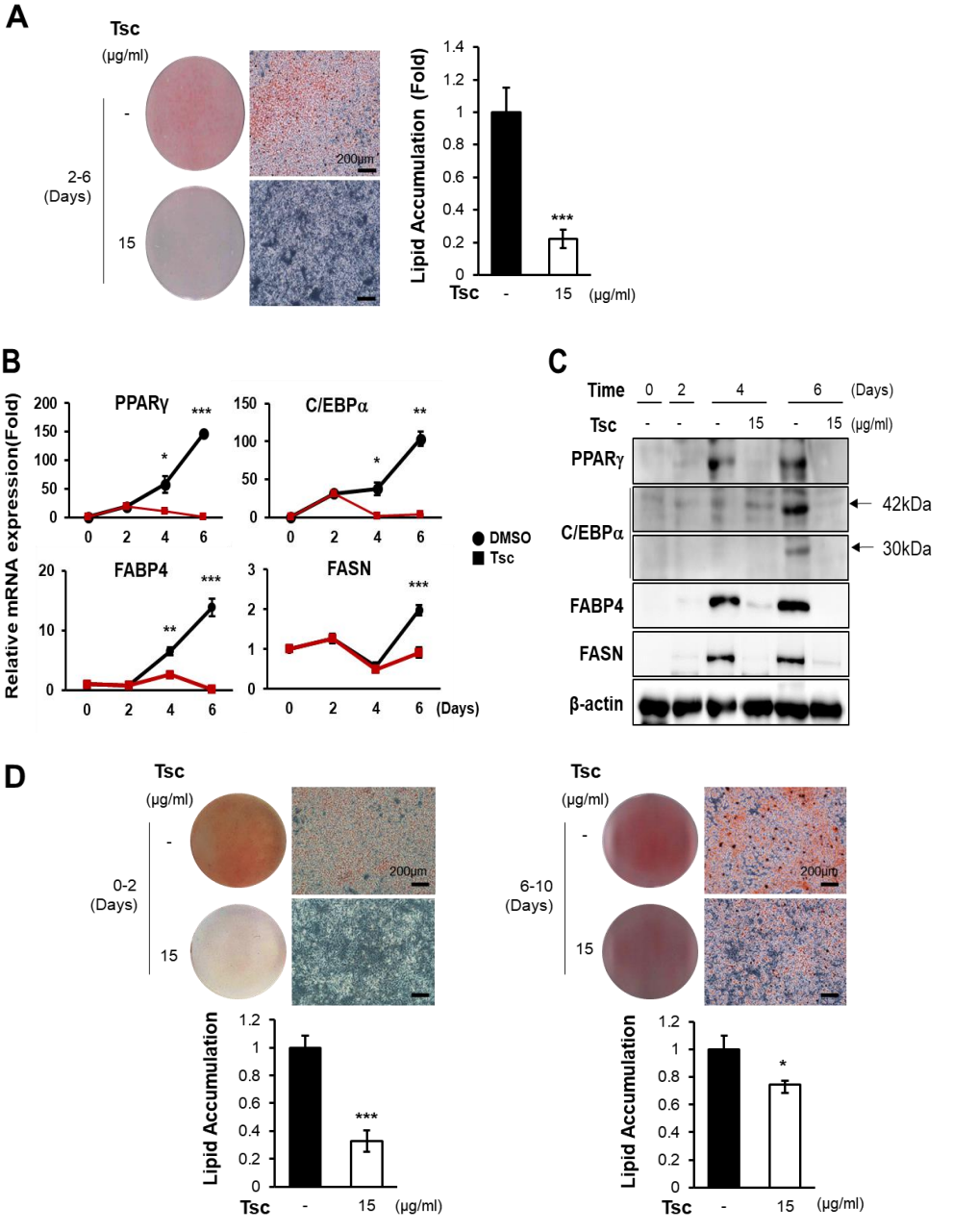

Figure 5. Tschimganidine reduces the expression levels of adipogenesis-related factors after adipocyte differentiation. (A) ORO

staining of tschimganidine-treated 3T3-L1 cells. After MDI induction, 3T3-L1 cells were treated with tschimganidine on days 2 to 6. ORO staining was performed on day 6. ORO was eluted with 100% isopropanol from stained cells, and the absorbance at 500 nm were measured. (B) mRNA expression of PPARγ, C/EBPα, FABP4, and FASN was detected using real-time polymerase chain reaction. RNA samples were prepared on days 0, 2, 4, and 6. 3T3-L1 cells were treated with tschimganidine on days 2 to 6. mRNA expression was normalized to that of β-actin. $*P < 0.05$, $**P < 0.01$, and $***P < 0.001$; dimethyl sulfoxide versus tschimganidine. (C) Protein expression of PPARγ, C/EBPα, FABP4, and FASN was detected by western blotting. Protein samples were prepared on days 0, 2, 4, and 6. 3T3-L1 cells were treated with tschimganidine on days 2 to 6. Protein expression was normalized to that of β-actin. (D) ORO staining and lipid accumulation in tschimganidine-treated 3T3-L1 cells. 3T3-L1 cells were treated with MDI and tschimganidine on day 2 (left panel). ORO staining was performed on day 6. 3T3-L1 cells were treated with tschimganidine on days 6 to 10 (right panel). ORO staining was performed on day 10. ORO, Oil Red O; MDI, methylisobutylxanthine–dexamethasone–insulin.

6. Tschimganidine induces the phosphorylation of AMP-activated kinase (AMPK) and Acetyl-CoA carboxylase (ACC)

Cell signaling molecules, such as AKT, AMPK, ERK, and JAK2, participate in adipogenesis and lipid accumulation[24]. To determine the molecular mechanisms by which tschimganidine affects adipogenesis and lipid accumulation, I assessed the changes in the activation of these signaling pathways from day 2 to 3 of adipocyte differentiation (Fig. 6A). The expression levels of AKT, AMPK, ERK 1/2, and JAK2 remained unaffected by tschimganidine treatment. However, the levels of p-AKT, ERK 1/2, and JAK2 were significantly lowered after tschimganidine treatment. Tschimganidine also increased AMPK phosphorylation. These results indicate that tschimganidine reduced the phosphorylation of adipogenesis-related signaling pathways during the early stages of adipocyte differentiation. Moreover, tschimganidine treatment increased AMPK and ACC phosphorylation in a time-dependent manner (Fig. 6B). Multiple studies have shown that AMPK is activated by phosphorylation and inhibits adipocyte differentiation[25-27].

I examined whether tschimganidine inhibits lipid accumulation through AMPK activation. The inhibitory effect of tschimganidine on lipid accumulation was reduced by the knockdown of AMPK gene expression using AMPK siRNAs. ORO staining, lipid droplet size, and lipid accumulation in the tschimganidine-treated 3T3-L1 cells after AMPK knockdown were lower than those in the control cells (Fig. 6C). Moreover, AMPK knockdown reduced the inhibitory effect of tschimganidine on the expression of genes related to adipogenesis and lipid accumulation (Fig. 6D). Thus, tschimganidine inhibits adipogenesis and lipid accumulation via AMPK activation.

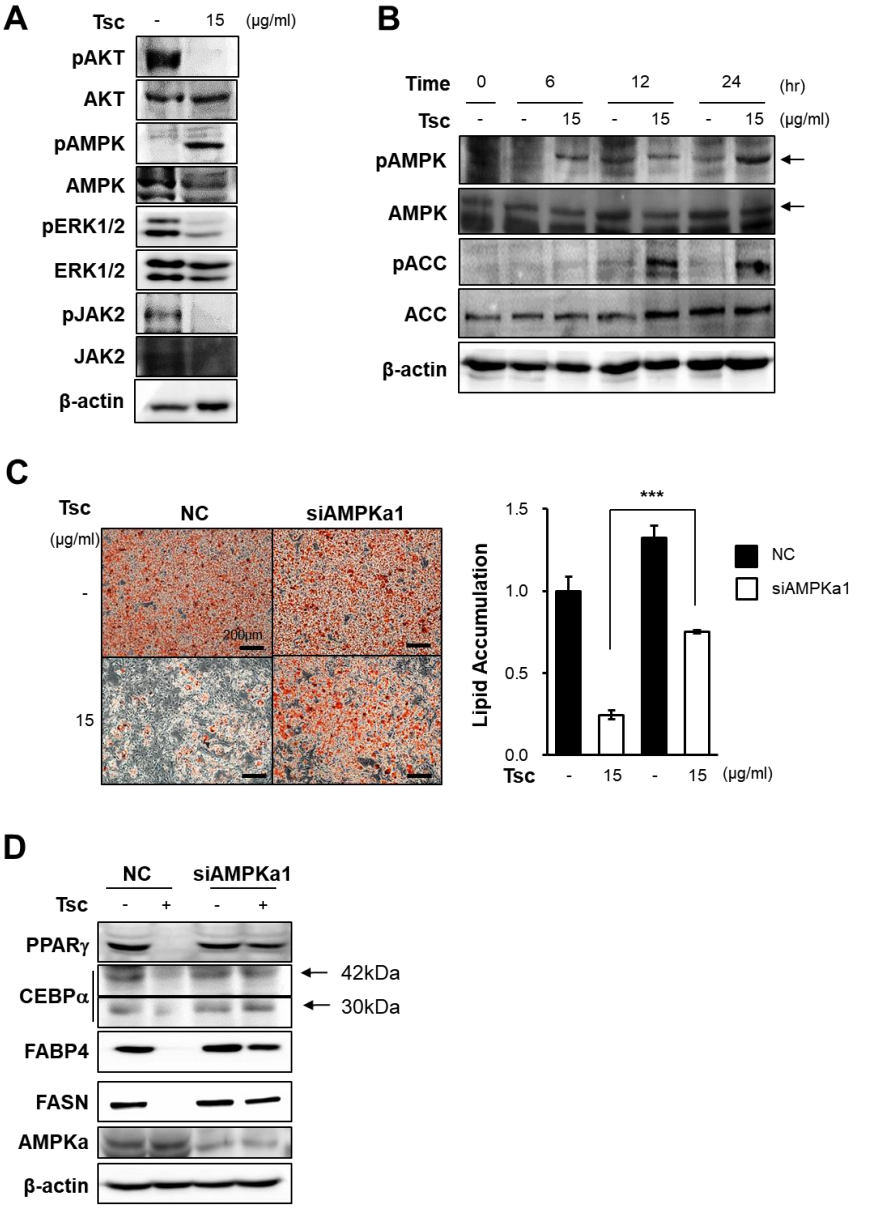

Figure 6. Tschimganidine induces the phosphorylation of AMP-activated kinase (AMPK) and Acetyl-CoA carboxylase (ACC). (A) Western blotting of signal transduction-related proteins. 3T3-L1 cells were treated with tschimganidine on day 2 and incubated for 24 h. (B) The activity of signal

transduction-related proteins, such as AMPK and ACC, was detected by western blotting. 3T3-L1 cells were treated with tschimganidine on day 2. (C) ORO staining and lipid accumulation in AMPKa1 knockdown 3T3-L1 cells with or without tschimganidine. After transfection of AMPKa1 small interfering RNA (siRNA), 3T3-L1 cells were differentiated using MDI. Following this, 3T3-L1 cells were treated with tschimganidine on day 2. ORO staining was performed on day 6. ORO was eluted with 100% isopropanol from the stained cells, and the absorbance at 500 nm was measured. ***$P < 0.001$; scRNA versus siAMPK. (D) Protein expression of PPARγ, C/EBPα, FABP4, and FASN was detected by western blotting. Protein samples were prepared on day 4. Protein expression was normalized to that of β-actin. ORO, Oil Red O; DMSO, dimethyl sulfoxide; MDI, methylisobutylxanthine–dexamethasone–insulin.

7. Tschimganidine affects body weight, insulin tolerance, and glucose tolerance in HFD-fed mice

The anti-obesity effects of tschimganidine were evaluated *in vivo*. Mice were fed an NFD or HFD (containing 60% of the total kcal as fat) for 12 weeks, and intraperitoneal injection of tschimganidine was started 5 weeks after feeding the HFD. Tschimganidine treatment reduced the body size of HFD-fed obese mice; however, no difference was noted in the body size of NFD-fed mice, regardless of tschimganidine treatment (Fig. 7A). The reduction in body weight was notable in HFD-fed mice (Fig. 7B). In particular, the mice treated with 5 μg/kg tschimganidine had a lower body weight than the control mice. However, no significant differences in food intake were noted between the NFD and HFD groups (Fig. 7C).

The effect of tschimganidine on metabolic parameters, such as ALT, glucose, and TG levels, were evaluated in the sera of experimental mice. Tschimganidine reduced the levels of ALT, glucose, and TG in the HFD-fed mice (Fig. 7D). I also assessed whether tschimganidine improves glucose homeostasis *in vivo*. Compared with the control mice, tschimganidine treatment significantly improved glucose tolerance in the HFD-fed mice (Fig. 7E). Insulin sensitivity was analyzed using the ITT. No differences were noted in blood glucose levels between the tschimganidine-treated and control NFD-fed mice; however, the blood glucose level was lower in the tschimganidine-treated HFD-fed mice than in the control HFD-fed mice (Fig. 7F). These data indicate that tschimganidine delays the increase in body weight and improves metabolic parameters such as ALT, blood glucose, and TG levels; insulin tolerance; and glucose tolerance in HFD-fed mice.

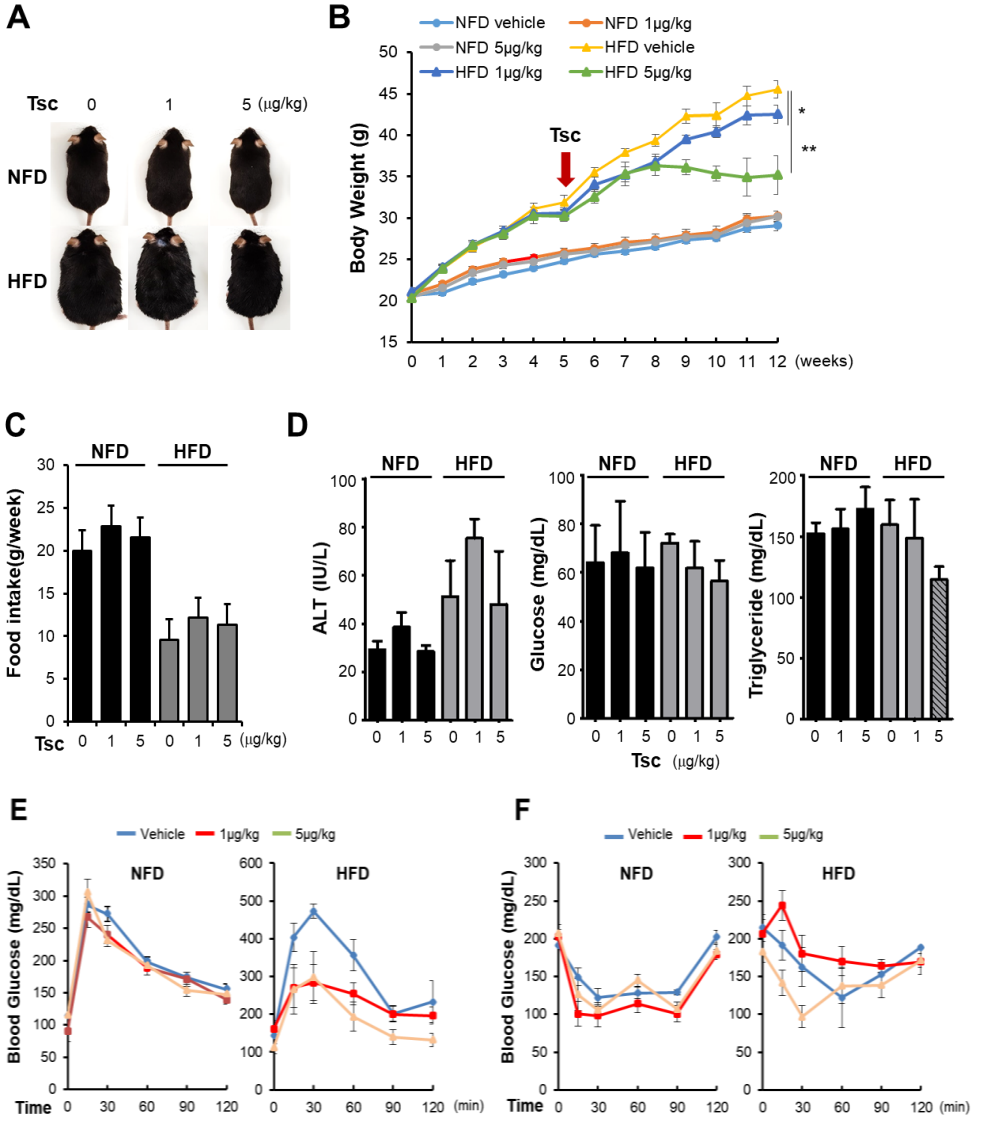

Figure 7. Tschimganidine affects body weight, insulin tolerance, and glucose tolerance in HFD-fed mice. (A, B) Reduced body size and weight of HFD-fed mice treated with tschimganidine for 12 weeks. Tschimganidine was administered to both HFD-fed and NFD-fed mice. Body weight was recorded every 2 days. *P < 0.05, **P < 0.01; n = 6 per group. (C) Food intake was

measured by weighing the remaining chow. (D) Measurement of ALT, glucose, and triglyceride levels. Blood was drawn and analyzed from the NFD- or HFD-fed mice with or without tschimganidine treatment. (E, F) Glucose tolerance test and insulin tolerance test. Vehicle (DMSO)- or tschimganidine (1 or 5 μg/kg)-treated mice. Blood glucose levels were measured at 15, 30, 60, 90, and 120 min. *$P < 0.05$, **$P < 0.01$; n = 6 per group of NFD-fed mice and n = 5 per group of HFD-fed mice. vehicle versus 5 μg/kg tschimganidine. NFD, normal-fat diet; HFD, high-fat diet; DMSO, dimethyl sulfoxide, ALT, alanine aminotransferase.

8. Tschimganidine reduces adipocyte size and adipogenesis-related factors in fat tissues of HFD-fed mice

The amount of gWAT and iWAT in NFD- and HFD-fed mice with or without tschimganidine treatment was evaluated. The amounts of gWAT and iWAT were reduced in the tschimganidine-treated HFD-fed obese mice (Fig. 8A). The tschimganidine-treated HFD-fed mice had lower gWAT and iWAT weights than the control mice (Fig. 8B). H&E staining of paraffin-embedded gWAT samples was performed for histological analysis. Significantly more adipocytes exhibited reduced size in the gWAT of the tschimganidine-treated NFD-fed and HFD-fed mice (Fig. 8C). Similarly, the tschimganidine-treated mice in both NFD-fed and HFD-fed groups had smaller adipocytes in the iWAT than the untreated control mice (Fig. 8D).

The mRNA expression of FABP4, PPARγ, C/EBPα, and FASN, which are markers of adipogenesis and lipid accumulation in the gWAT and iWAT, was assessed. The mRNA expression levels of FABP4, PPARγ, C/EBPα, and FASN were reduced in the gWAT of the tschimganidine-treated NFD-fed and HFD-fed mice (Fig. 8E). Similarly, tschimganidine inhibited the mRNA expression of FABP4, PPARγ, C/EBPα, and FASN in the iWAT of the HFD-fed mice (Fig. 8F). Tschimganidine also decreased C/EBPα and FASN expression levels in the iWAT of the NFD-fed mice. Taken together, tschimganidine reduced the weight and cell size of the gWAT and iWAT by downregulating adipogenesis-associated gene expression.

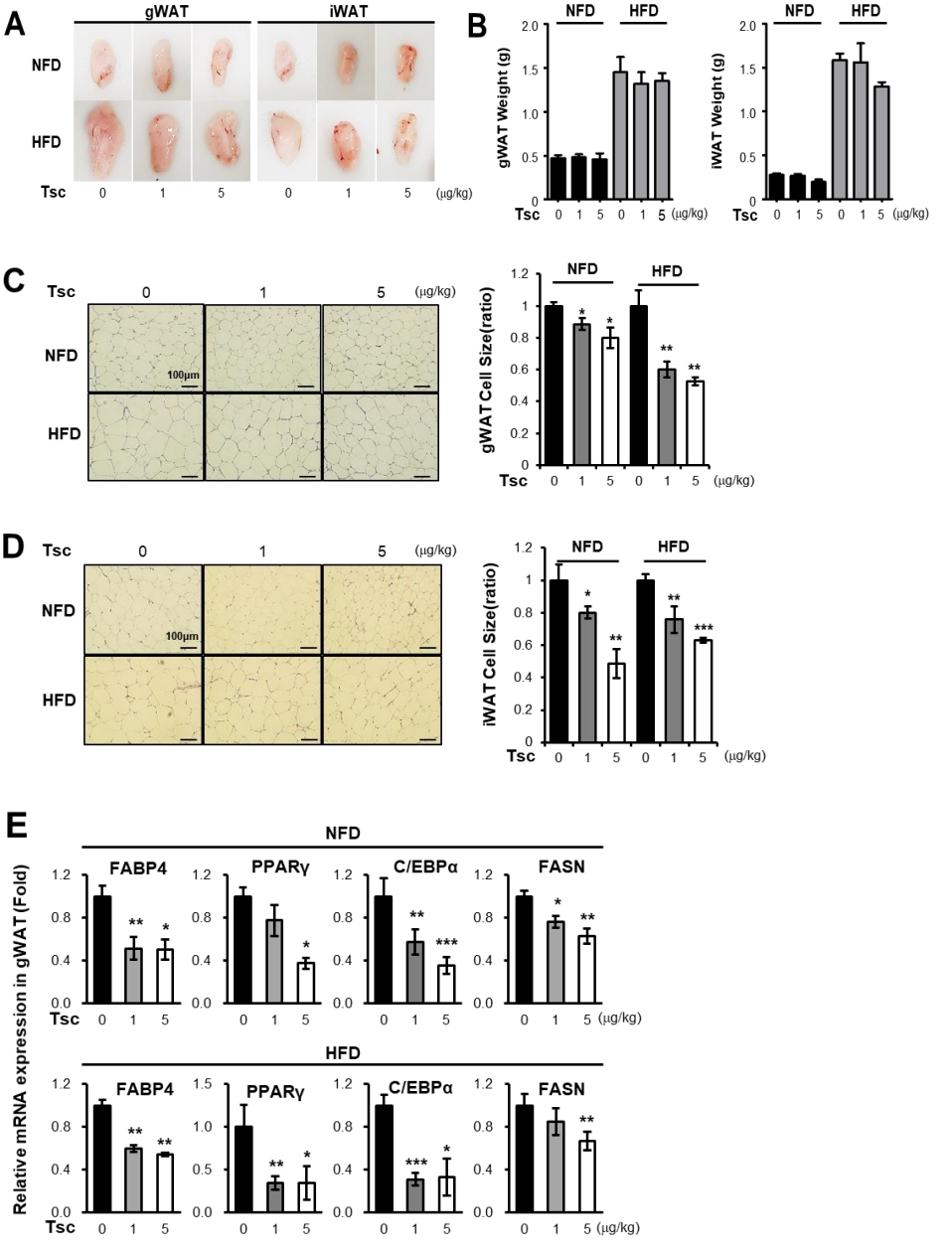

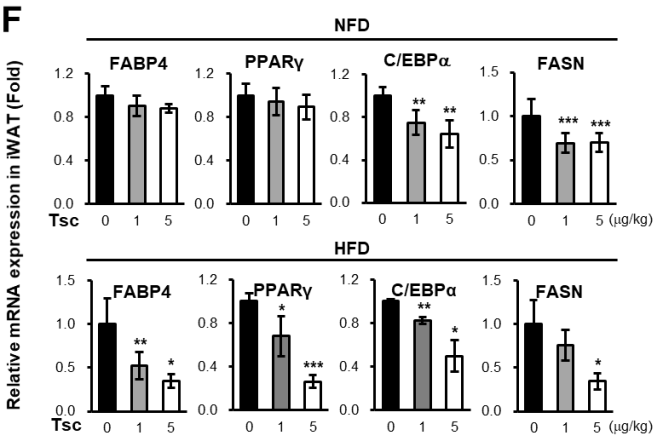

Figure 8. Tschimganidine reduces adipocyte size and adipogenesis-related factors in fat tissues of HFD-fed mice. (A) White adipose tissues of NFD- or HFD-fed mice administered vehicle (DMSO) or tschimganidine. (B) Gonadal and inguinal WAT weight was measured after the 12-week dietary period. (C) The adipocyte size of gonadal WAT sections was measured by H&E staining. Size measurements were performed using ImageJ software. (D) The adipocyte size of inguinal WAT sections was measured by H&E staining. Size measurements were performed as described above. (E, F) Gonadal and inguinal WATs were collected, and tissue lysates were prepared. mRNA expression of FABP4, PPARγ, C/EBPα, and FASN was assessed by real-time PCR analysis. β-actin was used as a normalization control. Data are presented as the mean ± SD; **P* < 0.05, ***P* < 0.01, and ****P* < 0.001 for vehicle versus 1 and 5 μg/kg tschimganidine treatment. H&E, hematoxylin and eosin; WAT, white adipose tissue; NFD, normal-fat diet; HFD, high-fat diet; PCR, polymerase chain reaction; DMSO, dimethyl sulfoxide.

9. Tschimganidine reduces steatosis in liver tissues of HFD-fed mice

I assessed whether tschimganidine inhibits lipid accumulation in the liver tissues of NFD-fed- and HFD-fed mice. The liver size was reduced in the tschimganidine-treated HFD-fed obese mice (Fig. 9A). The liver weight of the tschimganidine-treated mice was also lower than that of the control mice in the HFD-fed group (Fig. 9B). Next, I conducted H&E staining of paraffin-embedded liver tissues. Lipid accumulation in liver tissues was significantly reduced in the tschimganidine-treated HFD-fed mice (Fig. 9C). Hepatic TG and FFA levels were significantly lower in the tschimganidine-treated mice than in the control mice (Fig. 9D). Additionally, mRNA levels of lipid accumulation-related factors, such as FABP4, PPARγ, and FASN, were reduced in liver tissues of the tschimganidine-treated NFD-fed mice (Fig. 9E). Similar to the NFD-fed mice, tschimganidine repressed the gene expression of FABP4, PPARγ, and FASN in the liver of the HFD-fed mice (Fig.9F). Taken together, tschimganidine alleviated hepatic steatosis in HFD-fed mice.

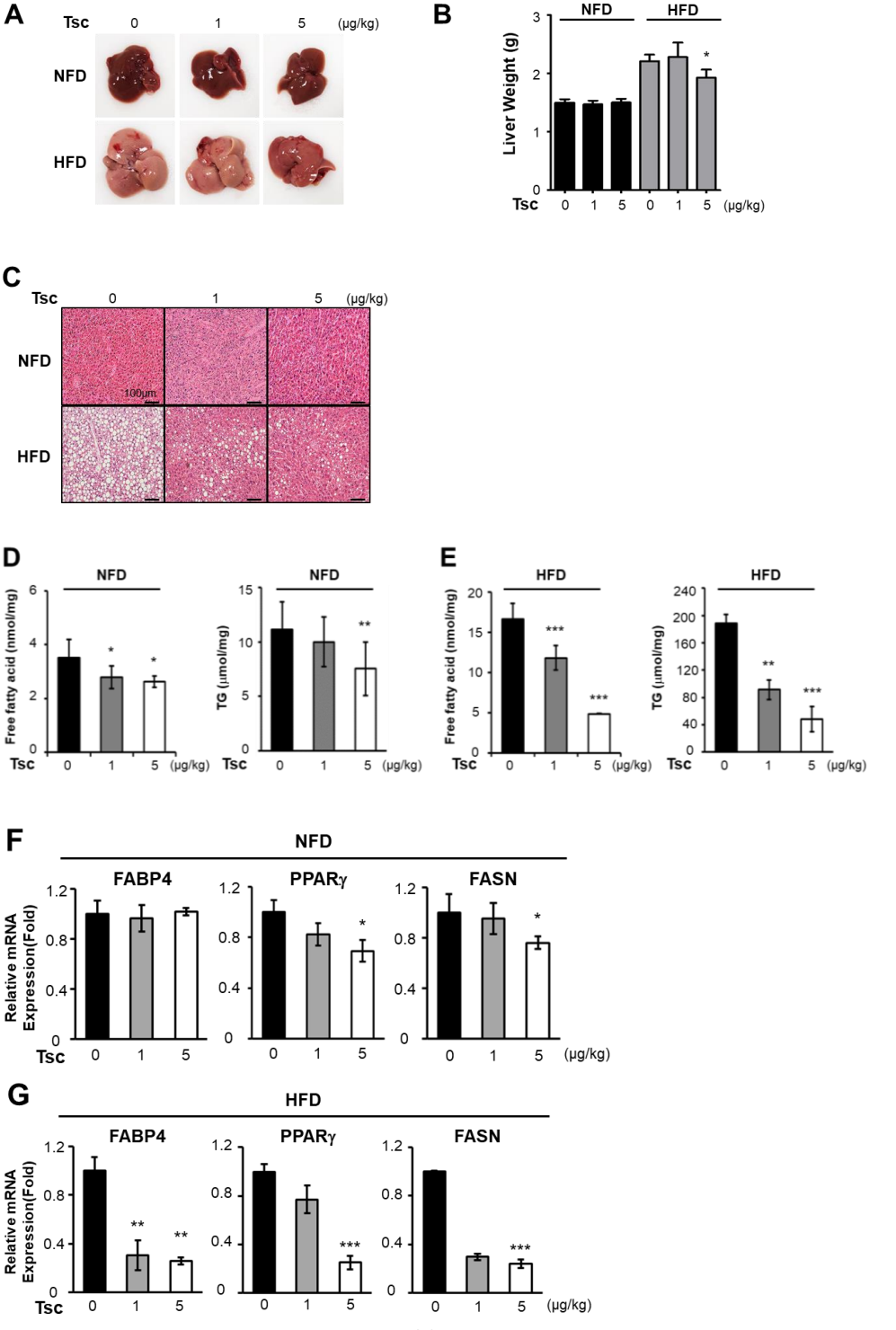

Figure 9. Tschimganidine reduces steatosis in liver tissues of high-fat diet-fed mice. (A, B) The size and weight of liver tissues from NFD- or HFD-fed mice. Liver weight was measured after the 12-week dietary period. (C) H&E staining of liver sections was performed in each group treated with or without tschimganidine for 10 weeks. (D) Hepatic TG and FFA levels. TG and FFA from the liver were extracted, and their levels were measured using the colorimetric method at 570 nm. (E, F) Liver tissue lysates were prepared, and the mRNA expression of FABP4, PPARγ, and FASN was assessed by real-time PCR. β-actin was used as a normalization control. Data are presented as the mean ± SD. **P* < 0.05, ***P* < 0.01, and ****P* < 0.001 for vehicle versus 1 and 5 μg/kg tschimganidine treatment. NFD, normal-fat diet; HFD, high-fat diet; FFA; free fatty acid, TG, triglyceride; PCR, polymerase chain reaction.

IV. DISCUSSION

Obesity is one of the most common metabolic diseases[28]. According to statistics from the World Health Organization, 39% of adults aged 18 years and older were overweight in 2016, and 13% were obese. Obesity results in diabetes, heart diseases and cancer[29-31]. Therefore, the development of therapeutic agents to manage and treat obesity is urgently required.

Notch signaling is related to adipogenesis and lipid accumulation[11] and plays important roles in immune cells[12]. ATM, one of the immune cells, is rich in adipose tissues and is known to participate in lipid metabolism and lipid-mediated inflammation[6]. Therefore, I intended to elucidate the molecular mechanism by which Hes1, a target of the Notch signaling pathway, affects macrophages in adipose tissues. Under HFD conditions, the macrophage population increased in the eWAT and the expression levels of Notch signaling genes, including the Hes1 gene, increased in ATMs. I also confirmed that Notch signaling was activated in macrophages upon contact with adipocytes and not by a soluble factor secreted by adipocytes. In addition, using myeloid-specific Hes1 cKO mice, I found that Hes1 deletion increased resistance to HFD-induced obesity. Body weight and metabolic fitness were ameliorated in the HFD-fed Hes1 cKO mice. H&E staining revealed that the Hes1 cKO mice had smaller lipid droplets in adipose tissues and liver. Furthermore, the Hes1 cKO mice had lower blood glucose levels over the entire period of the GTT and ITT. The contents of ALT (a marker of liver toxicity), serum glucose, total cholesterol, and FFA were decreased in the Hes1 cKO mice. These results propose that Hes1 is associated with obesity and has the potential to be a therapeutic target for managing obesity and metabolic diseases.

I next investigated the differences in gene expression between the Wild-type and Hes1 cKO mice by performing RNA sequencing. When Hes1 cKO BMDMs in contact with differentiated adipocytes, Hes1 cKO BMDMs

exhibited approximately threefold higher expression levels of the IL-10 gene than wild-type BMDMs. This result was also observed by performing real-time PCR. IL-10 expression was significantly increased in Hes1-deleted THP-1 cells. IL-10 is an anti-inflammatory cytokine secreted by M2 macrophages in the adipose tissue[23]. M2 macrophages maintain insulin sensitivity through the anti-inflammatory actions of IL-10 and signal transducer and activator of transcription (STAT)-3[23]. IL-10 exhibits various anti-inflammatory effects in macrophages and can effectively inhibit inflammation and autoimmune diseases[32]. IL-10 also promotes insulin signaling in adipocytes by directly suppressing the synthesis of inflammatory cytokines, such as TNF-α. Moreover, it prevents the effects of TNF-α on blocking insulin-stimulated glucose uptake in adipocytes[33]. Our *in vitro* studies revealed that IL-10 (10 ng/mL) repressed the expression of adipogenesis- and lipid accumulation-related genes, such as those encoding FABP4, FASN, and C/EBPα. Furthermore, I confirmed that IL-10 reduced lipid accumulation in a dose-dependent manner and that IL-10 exhibited an inhibitory effect on adipogenesis at the early stage of adipocyte differentiation. These data suggest that Hes1 depletion in macrophages increases IL-10 expression and can reduce inflammation in the adipose tissue, and inhibit adipocyte differentiation and fat accumulation.

Next, I focused on natural products to identify a therapeutic agent that exhibits a similar effect to Hes1 inhibition. Natural products are composed of bioactive phytochemicals with beneficial health effects, and they can help treat obesity and metabolic diseases despite their safety concerns[16-19]. Previously, I performed a screening analysis to identify natural compounds with anti-obesity effects[34]. I found that tschimganidine, a terpenoid, exhibited the expected effect of inhibiting lipid accumulation in 3T3-L1 cells. Tschimganidine is a member of the Umbelliferae family[16]. Terpenoids have been reported to be selectively toxic against gram-positive bacteria[35] and exhibit anti-cancer effects[36]. However, there are only two reports on the biological activity of tschimganidine: it can act

as an agonist of estrogen receptor-alpha (ERα)[37] and extend the lifespan of yeast[38]. Tschimganidine can also act as a phytoestrogen[39]. Phytoestrogens are natural phytochemicals that have a function similar to that of gonadal estrogen hormones and are potential alternatives to hormone replacement therapy[16]. Among phytoestrogens, terpenoids can exhibit both estrogenic and anti-estrogenic activities by targeting estrogen receptors[40]. In particular, tschimganidine functions as an ERα agonist and has estrogen-mimicking characteristics[37]. ERα agonists have been reported to exhibit anti-obesity effects by stimulating estrogen receptors[41]. However, research on these effects of terpenoids was lacking; therefore, it is worthwhile to conduct a study on how tschimganidine affects obesity.

I hypothesized that tschimganidine can be effective in natural product-derived therapy by inhibiting Notch signaling and adipogenesis. In this study, I found that treatment with tschimganidine suppressed Notch signaling factors, including Hes1, and upregulated IL-10 expression. Moreover, tschimganidine drastically reduced the expression of adipogenesis-associated genes, such as those encoding PPARγ, C/EBPα, FASN, and FABP4 and reduced adipogenesis in 3T3-L1 cells. These results were confirmed using tschimganidine at a concentration that maintains cell viability. I proposed that the anti-adipogenic effect of tschimganidine is due to the reduced expression of these genes. I determined the optimal concentration of tschimganidine that can suppress adipogenesis. Cells treated with 15 μg/mL tschimganidine displayed inhibited differentiation and reduced lipid accumulation, as revealed by ORO staining. I confirmed that the expression of adipogenesis-associated genes was significantly reduced. I also observed this effect *in vivo*. Tschimganidine reduced obesity in HFD-fed mice. The expression of lipid accumulation- and adipogenesis-associated genes, such as those encoding FABP4, PPARγ, C/EBPα, and FASN, was significantly decreased in the WATs of these mice. Hence, I hypothesized that tschimganidine, a phytoestrogen, inhibits the

expression of adipogenesis-associated genes.

I further noted a significant increase in the phosphorylation of AMPK following tschimganidine treatment. AMPK is a heterotrimeric enzyme that plays a major role in maintaining energy homeostasis in various organs and tissues[42]. In the adipose tissue, it has been reported to play an important role in regulating adipocyte glucose and lipid metabolism[43]. When AMPK is activated, it induces the phosphorylation of downstream signaling targets either directly or indirectly. This decreases the synthesis of cholesterol and fatty acids[44]. Regulation of lipid metabolism is a well-known function of AMPK. AMPK also acts as a cellular sensor of glycogen, which regulates the rate of synthesis and breakdown of this fuel source[45]. AMPK is activated by stresses that cause adenosine triphosphate (ATP) depletion, leading to increased binding of adenosine monophosphate (AMP) and adenosine diphosphate (ADP) to specific regulatory sites of this kinase. This results from ATP hydrolysis, which is rapidly converted to AMP by the adenylate kinase reaction[43]. The activation of ERα induces AMPK phosphorylation, which increases beiging of white adipocytes[46]. Therefore, I investigated whether tschimganidine induces AMPK phosphorylation and found that the activation of AMPK by tschimganidine increases adipocyte lipolysis, despite the debate regarding whether AMPK could play a role in regulating lipolysis[47-48]. Tschimganidine increased the phosphorylation of AMPK, accompanied by the phosphorylation of ACC. However, the effect of tschimganidine treatment on the inhibition of lipid accumulation was diminished by the knockdown of AMPK gene expression. This indicates that the effect of tschimganidine on lipid accumulation was based on the activation of AMPK, which is the predominant mechanism by which tschimganidine affects adipogenesis and lipid accumulation as an ERα agonist.

Furthermore, tschimganidine improved glucose tolerance and insulin resistance in HFD-fed mice. Our results support that tschimganidine increases AMPK activation and induces blood glucose uptake and lipolysis in adipose

tissues. Lipid contents were significantly reduced in the liver tissues of HFD-fed mice. Tschimganidine treatment reduced TG and FFA levels in the liver and lowered the expression of lipid accumulation-associated genes in liver tissues, suggesting that tschimganidine is beneficial in treating fatty liver and related metabolic diseases. Our results indicate that tschimganidine may act as an effective therapeutic agent against obesity and metabolic diseases by inhibiting adipogenesis through the activation of AMPK. However, further research is needed to determine the detailed mechanism, including which proteins tschimganidine targets and how this modulates AMPK activity.

In summary, Hes1 deletion in macrophages exerts an anti-obesity effect in adipose tissues by increasing IL-10 expression. Moreover, tschimganidine, an inhibitor of Notch signaling, reduces adipogenesis, lipid accumulation, and blood glucose levels through the activation of AMPK. Tschimganidine is a potential therapeutic agent against obesity and metabolic diseases. Further mechanistic studies are needed to evaluate its clinical application.

V. CONCLUSION

The level of Hes1 was elevated in the ATMs of HFD-fed obese mice. Moreover, the Hes1 level was increased in BMDMs upon contact with differentiated adipocytes. After 12 weeks of HFD feeding, Hes1 deficiency reduced obesity in the mice and lowered the lipid droplet size and inflammation in the adipose tissue. When the blood glucose level in the wild-type and Hes1 cKO mice was measured by GTTs and ITTs, the glucose level of the Hes1 cKO mice was found to be lowered. In addition, the level of ALT, an indicator of liver toxicity, was lowered. Metabolic fitness was also ameliorated in the Hes1 cKO mice. RNA sequencing analysis revealed that the expression level of the IL-10 gene related to anti-inflammation was elevated in BMDMs upon contact with differentiated adipocytes. The increased level of IL-10, a cytokine derived from macrophages, was confirmed by real-time PCR. IL-10 suppressed adipogenesis and lipid accumulation in adipocytes. Tschimganidine, belonging to the Umbelliferae family, exhibited anti-obesity effects through inhibiting Notch signaling and upregulating IL-10 gene expression. Tschimganidine treatment reduced the expression of adipogenesis- and lipid accumulation-related genes such as those encoding FABP4, FASN, PPARγ and C/EBPα. After 12 weeks of HFD feeding, tschimganidine decreased obesity and the size of adipose tissues in the mice. It reduced lipid accumulation and lowered the expression of adipogenesis-associated genes in the WAT. Tschimganidine also reduced the hepatic FFA and TG levels under HFD conditions. Furthermore, it improved glucose homeostasis in mice. Tschimganidine appeared to inhibit adipogenesis and lipid accumulation via AMPK activation. Therefore, I suggest that Hes1 might be a therapeutic target against obesity and metabolic diseases. It can serve as a potential drug to manage and prevent obesity.

REFERENCES

1. Bray GA, Heisel WE, Afshin A, Jensen MD, Dietz WH, Long M et al. The Science of Obesity Management: An Endocrine Society Scientific Statement. Endocr Rev 2018; **39**: 79-132.
2. Velazquez A, Apovian CM. Updates on obesity pharmacotherapy. Ann N Y Acad Sci 2018; **1411**: 106-119.
3. Djalalinia S, Qorbani M, Peykari N, Kelishadi R. Health impacts of obesity. Pak J Med Sci 2015; **31**: 239-242.
4. Rosário M, Isabel A. Chronic inflammation in obesity and the metabolic Syndrome, mediators of Inflammation. Mediators Inflamm 2010; 2010; 289645.
5. Cho KW, Zamarron BF, Muir LA, Singer K, Porsche CE, DelProposto JB, et al. Adipose tissue dendritic cells are independent contributors to obesity-induced inflammation and insulin resistance. J Immunol 2016;197 (9): 3650-3661.
6. Dahik VD, Frisdal E, Le Goff W. Rewiring of Lipid Metabolism in Adipose Tissue Macrophages in Obesity: Impact on Insulin Resistance and Type 2 Diabetes. Int J Mol Sci 2020; 21(15): 5505.
7. Prieur X, Mok CY, Velagapudi VR, Núñez V, Fuentes L, Montaner D, et al. Differential lipid partitioning between adipocytes and tissue macrophages modulates macrophage lipotoxicity and M2/M1 polarization in obese mice. Diabetes 2011; 60: 797–809.
8. Shapiro H, Pecht T, Shaco-Levy R, Harman-Boehm I, Kirshtein B, Kuperman Y, et al. Adipose tissue foam cells are present in human obesity. J Clin Endocrinol Metab 2013; 98: 1173-1181.
9. Surabhi S, Tripathi BK, Maurya B, Bhaskar PK, Mukherjee A, Mutsuddi M. Regulation of Notch Signaling by an evolutionary conserved DEAD Box

RNA helicase, maheshvara in *Drosophila melanogaster*. Genetics 2015; 201: 1071-1085.

10. Chris S, Urban L. Notch signaling in development, tissue homeostasis, and disease. 2017; 94(4): 1234-1294.
11. Shan T, Liu J, Wu W, Xu Z, Wang Y. Roles of Notch signaling in adipocyte progenitor cells and mature adipocytes. J Cell Physiol 2017; 232: 1258-1261.
12. Shang Y, Smith S, Hu X. Role of Notch signaling in regulating innate immunity and inflammation in health and disease. Protein cell 2016; 7(3): 159-174.
13. Park JS, Kim SH, Kim K, Jin CH, Choi KY, Jang J, et al. Inhibition of notch signalling ameliorates experimental inflammatory arthritis. Ann Rheum Dis 2015; 74(1): 267-274.
14. Eagar TN, Tang Q, Wolfe M, He Y, Pear WS, Bluestone JA. Notch 1 signaling regulates peripheral T cell activation. Immunity 2004; 20(4): 407-415.
15. Kang JA, Kim WS, Park SG. Notch1 is an important mediator for enhancing of B-cell activation and antibody secretion by Notch ligand. Immunology 2014; 143(4): 550-559.
16. Prakash DG. Role of phytoestrogens as nutraceuticals in human health. In. Pharmacologyonline. vol. 1; 2011; pp 510-523.
17. Rousseaux CG, Schachter H. Regulatory issues concerning the safety, efficacy and quality of herbal remedies. Birth Defects Res B Dev Reprod Toxicol 2003; 68: 505-510.
18. Saad B, Kadan S, Shanak S, Zaid H. Anti-diabetes and anti-obesity Medicinal Plants and Phytochemicals: Safety, Efficacy, and Action Mechanisms. 1st edn; Springer International Publishing: Imprint: Springer: Cham; 2017; pp 1 online resource (XIV, 257 pages, 255 illustrations, 253 illustrations in color).

19. Seca AML, Pinto D. Plant Secondary Metabolites as Anticancer Agents: Successes in Clinical Trials and Therapeutic Application. Int J Mol Sci 2018; 19: 263.
20. Ho TT, Tran QT, Chai CL. The polypharmacology of natural products. Future Med Chem 2018; 10: 1361-1368.
21. Mary L, Cornelius JKG, Andjulian R. Yates III, Julian R. Toxicity of Monoterpenoids and Other Natural Products to the Formosan Subterranean Termite (Isoptera: Rhinotermitidae). J Econ Entomol 1997; 90: 320-325.
22. Schneider CA, Rasband WS, Eliceiri KW. NIH Image to ImageJ: 25 years of image analysis. Nat Methods 2012; 9: 671-675.
23. Appari M, Channon KM, Mcneill E. Metabolic regulation of adipose tissue macrophage function in obesity and diabetes. Antioxid Redox Signal 2018; 29(3): 297-312.
24. Guru A, Issac PK, Velayutham M, Saraswathi NT, Arshad A, Arockiaraj J. Molecular mechanism of down-regulating adipogenic transcription factors in 3T3-L1 adipocyte cells by bioactive anti-adipogenic compounds. Mol Biol Rep 2021; 48: 743-761.
25. Chen H, Zhang L, Li X, Li X, Sun G, Yuan X, et al. Adiponectin activates the AMPK signaling pathway to regulate lipid metabolism in bovine hepatocytes. J Steroid Biochem Mol Biol 2013; 138: 445-454.
26. Jeon SM. Regulation and function of AMPK in physiology and diseases. Exp Mol Med 2016; 48: e245.
27. Chen D, Wang Y, Wu K, Wang X. Dual Effects of Metformin on Adipogenic Differentiation of 3T3-L1 Preadipocyte in AMPK-Dependent and Independent Manners. Int J Mol Sci 2018; 19: 1547.
28. Engin A. The Definition and Prevalence of Obesity and Metabolic Syndrome. Adv Exp Med Biol 2017; 960: 1-17.
29. Pi-Sunyer X. The Medical Risks of Obesity. Postgrad Med 2009; 121: 21-33.

30. Gallagher EJ, LeRoith D. Obesity and diabetes: the increased risk of cancer and cancer-related mortality. Physio Rev 2015; 95: 727-48.
31. Hruby A, Manson JE, Qi L, Malik VS, Rimm EB, Sun Q, et al. Determinants and Consequences of Obesity. Am J Public Health 2016; 106: 1656-1662
32. Saraiva M, O'Garra A. The regulation of IL-10 production by immune cells. Nat Rev Immunol 2010, 10(3): 170-181.
33. Stolarczyk E. Adipose tissue inflammation in obesity: a metabolic or immune response? Current opin Pharmacol 2017; 37: 35-40.
34. Baek JH, Kim NJ, Song JK, Chun KH. Kahweol inhibits lipid accumulation and induces glucose-uptake through activation of AMP-activated protein kinase (AMPK). BMB Rep 2017; 50: 566-571.
35. Tamemoto K, Takaishi Y, Chen B, Kawazoe K, Shibata H, Higuti T et al. Sesquiterpenoids from the fruits of *Ferula kuhistanica* and antibacterial activity of the constituents of *F. kuhistanica*. Phytochemistry 2001; 58: 763-767.
36. Chen QF, Liu ZP, Wang FP. Natural sesquiterpenoids as cytotoxic anticancer agents. Mini Rev Med Chem 2011; 11: 1153-1164.
37. Ikeda K, Arao Y, Otsuka H, Nomoto S, Horiguchi H, Kato S et al. Terpenoids found in the umbelliferae family act as agonists/antagonists for ER(alpha) and ERbeta: differential transcription activity between ferutinine-liganded ER(alpha) and ERbeta. Biochem Biophys Res Commun 2002; 291: 354-360.
38. Stephan J, Franke J, Ehrenhofer-Murray AE. Chemical genetic screen in fission yeast reveals roles for vacuolar acidification, mitochondrial fission, and cellular GMP levels in lifespan extension. Aging Cell 2013; 12: 574-583.

39. Tripathi S, Srivastava S, Tripathi YB. Role of herbal nutraceuticals in prevention and treatment of atherosclerosis. Explor Anim Med Res 2019; 9: 15-23.
40. Kiyama R. Estrogenic terpenes and terpenoids: Pathways, functions and applications. Eur J Pharmacol 2017; 815: 405-415.
41. Kim SN, Ahn SY, Song HD, Kwon HJ, Saha A, Son Y et al. Antiobesity effects of coumestrol through expansion and activation of brown adipose tissue metabolism. J Nutr Biochem 2020; 76: 108300.
42. Antonioli L, Colucci R, Pellegrini C, Giustarini G, Sacco D, Tirotta E et al. The AMPK enzyme-complex: from the regulation of cellular energy homeostasis to a possible new molecular target in the management of chronic inflammatory disorders. Expert Opin Ther Targets 2016; 20: 179-191.
43. Ceddia RB. The role of AMP-activated protein kinase in regulating white adipose tissue metabolism. Mol Cell Endocrinol 2013; 366: 194-203.
44. Ahmad B, Serpell CJ, Fong IL, Wong EH. Molecular mechanisms of adipogenesis: the anti-adipogenic role of AMP-activated protein kinase. Front Mol Biosci 2020; 7: 76.
45. McBride A, Ghilagaber S, Nikolaev A, Hardie DG. The glycogen-binding domain on the AMPK beta subunit allows the kinase to act as a glycogen sensor. Cell Metab 2009; 9: 23-34.
46. Santos RS, Frank AP, Fatima LA, Palmer BF, Oz OK, Clegg DJ. Activation of estrogen receptor alpha induces beiging of adipocytes. Mol Metab 2018; 18: 51-59.
47. Hong SW, Lee J, Park SE, Rhee EJ, Park CY, Oh KW et al. Activation of AMP-activated protein kinase attenuates tumor necrosis factor-alpha-induced lipolysis via protection of perilipin in 3T3-L1 adipocytes. Endocrinol Metab (Seoul) 2014; 29: 553-560.

48. Szkudelski T, Szkudelska K. Effects of AMPK activation on lipolysis in primary rat adipocytes: studies at different glucose concentrations. Arch Physiol Biochem 2017; 123: 43-49.

ABSTRACT (IN KOREAN)

대식세포내의 Notch 신호전달이 대사성 질환에 미치는 영향에 관한 연구

<지도교수 전경희>

연세대학교 대학원 의과학과

황민선

비만은 고혈압, 심장병, 제 2형 당뇨병을 동반하기 때문에 사망률과 이환율 위험을 증가시키는 질병이다. 또한 지방 조직의 지질 축적은 염증을 유발하고 인슐린 저항성을 유발 할 수 있다. 따라서 비만치료를 위한 효과적인 분자적 메커니즘과 약물치료제 개발이 시급하다. 지방 조직의 대식세포와 같은 면역 세포가 항상성 조절에 중요한 역할을 할 것으로 예상되지만, 식이 유발 비만에서 지질이 지방 조직 대식세포 표현형을 형성하는 기전에 대해서는 여전히 추가 연구가 필요하다. 다양한 세포 기능을 조절하는 Notch 신호 전달 체계와 염증 반응 사이의 연관성은 많은 연구에서 뒷받침되고 있으며, Notch 신호 전달은 염증 신호에 의해 조절된다. Hes1은 Notch 신호 전달 체계의 대표적인 타겟 중 하나로 대식세포의 TLR 반응을 부정적으로 조절하여 Hes1이 잠재적으로 자가 면역 및 염증성 장애에 관련되어 있음을 시사한다. 따라서 비만과 염증에 관련하여 Hes1, 대식 세포, 지방 조직 사이에 어떤 연관성이 있다는 가설을 세웠다.

본 논문에서 비만 마우스의 면역세포에서 Notch 신호 인자들이 증가함을 확인했다. 대식세포 특이적으로 Hes1을 저해한 (Hes1 cKO) 마우스에 고지방 식이를 먹였을 때, cKO 마우스는 체중이 덜 증가하며, 혈당이 감소하는 것을 관찰했다. 또한 cKO 마우스의 골수

유래 대식세포 (BMDM)의 항염증성 사이토카인인 IL-10 발현 수준은 지방세포의 지질과 접촉했을 때 증가했고, IL-10은 지방세포의 지방 생성과 지질 축적을 억제하였다. 게다가 Umbelliferae family의 terpenoids인 Tschimganidine이 대식세포에서 Notch 신호 인자들과 Hes1을 억제한다는 것을 발견했다. Tschimganidine 처리는 AMP-활성 단백질 키나제 (AMPK) 활성화를 통해 지방 생성 및 지질 축적 관련 인자들의 유전자 발현 수준 감소를 통해 지질 축적 및 지방 생성을 감소시켰다. 따라서 이러한 결과들에 따르면, 대식세포의 Hes1은 지방 조직에서 중요한 역할을 하며 대사성 질환에 영향을 미치는 것으로 보인다. 결과적으로 Hes1이 비만과 대사성 질환에 대한 치료 타겟이 될 수 있으며, Hes1의 억제제인 tschimganidine이 지방 생성을 억제하고 포도당 항상성을 향상시키는 잠재적인 항비만제임을 제안한다.

핵심되는 말 : 비만, Notch 신호, Hes1, 대식세포, 천연물치료제